

## Exergo-economic comparison of waste heat recovery cycles for a cement industry case study

José J. Fierro<sup>a,1</sup>, Cristian Hernández-Gómez<sup>a</sup>, Carlos A. Marengo-Porto<sup>a,2</sup>, César Nieto-Londoño<sup>a,\*,3</sup>, Ana Escudero-Atehortua<sup>a,4</sup>, Mauricio Giraldo<sup>b</sup>, Hussam Jouhara<sup>c,5</sup>, Luiz C. Wrobel<sup>c,6</sup>

<sup>a</sup> Escuela de Ingenierías, Universidad Pontificia Bolivariana, Medellín, Colombia

<sup>b</sup> Cementos Argos, Medellín, Colombia

<sup>c</sup> College of Engineering, Design and Physical Sciences, Brunel University London, London, England, United Kingdom

### ARTICLE INFO

#### Keywords:

Waste heat recovery  
Cement kiln effluent  
Exergo-economic analysis  
Emissions savings  
Decision making

### ABSTRACT

This work evaluates the performance regarding exergo-economic and emissions requirements of Waste Heat Recovery configurations (Organic Rankine cycle, Trilateral flash cycle, and Kalina cycle) under different operating conditions and working fluids. It was found that the best economic performance is presented by the Organic Rankine cycle that operates with Cyclo-Pentane and has two intermediate heat exchangers since it pushes the expansion temperature up while allowing a higher heat input to the cycle. As a result, it delivers 6.2 MW with a net present value, the net present value of 0.74 million dollars, saving up to 11480 tonnes of carbon dioxide per year. This performance far exceeds that obtained in the previous work, around 50% higher net-work with 80% higher net present value, and constitutes the best alternative in terms of performance to recover waste heat from the source evaluated. Regarding the Trilateral flash cycle, it can be stated that the net work and the exergetic performance are independent of the working fluid as long as there is not a very large volume change in the expander. The Kalina cycle presents slight exergy destruction, but the power delivered does not compensate for the high total capital cost due to the high pressures that must be handled, 55–120 bar, compared to the Organic Rankine cycle, 4–40 bar. An approach was made to more realistic cases where the methodology used facilitates selecting the best alternative when there is a budget restriction using the total capital cost and net work alternatively like a fixed requirement and net present value as the primary decision criterion.

### Introduction

In the last century, cement has become the second most consumed products in the world after water [1]. Cement production is intensive in energy usage as well as in CO<sub>2</sub> emissions [2]. It is also responsible for more than 5% of all human-made Green House Gas emissions (GHGs) [3]. Clinker, an intermediate compound in cement production, is obtained through the calcination of raw meal, mainly limestone, at

sintering temperatures in large rotary kilns. The pre-heating, pre-calcination and the kiln itself account for more than 50% of the direct GHGs from chemical processes, that is, the decarbonisation reaction of limestone, which produces CO<sub>2</sub>. Prices dominate the cement market since quality is strictly standardised and regulated, creating barriers to change its composition. Around 40% of the fuel-burning in the manufacturing of cement occurs directly in the kiln, this means that the costs associated with the energy consumption in this unit are equivalent to 35–45% of total production costs [1]. It is estimated that 40% of the energy demand

\* Corresponding author.

E-mail addresses: [jose.fierro@upb.edu.co](mailto:jose.fierro@upb.edu.co) (J.J. Fierro), [carlos.manrecop@upb.edu.co](mailto:carlos.manrecop@upb.edu.co) (C.A. Marengo-Porto), [cesar.nieto@upb.edu.co](mailto:cesar.nieto@upb.edu.co) (C. Nieto-Londoño), [mgiraldogir@argos.com.co](mailto:mgiraldogir@argos.com.co) (M. Giraldo), [hussam.jouhara@brunel.ac.uk](mailto:hussam.jouhara@brunel.ac.uk) (H. Jouhara), [luz.wrobel@brunel.ac.uk](mailto:luz.wrobel@brunel.ac.uk) (L.C. Wrobel).

<sup>1</sup> ORCID ID: <https://orcid.org/0000-0003-2306-611X>

<sup>2</sup> ORCID ID: <https://orcid.org/0000-0002-2969-5040>

<sup>3</sup> ORCID ID: <https://orcid.org/0000-0001-6516-9630>

<sup>4</sup> ORCID ID: <https://orcid.org/0000-0003-2962-4426>

<sup>5</sup> ORCID ID: <https://orcid.org/0000-0002-6910-6116>

<sup>6</sup> ORCID ID: <https://orcid.org/0000-0001-6702-0178>

<https://doi.org/10.1016/j.ecmx.2022.100180>

Available online 10 January 2022

2590-1745/© 2022 The Authors.

Published by Elsevier Ltd.

This is an open access article under the CC BY-NC-ND license

(<http://creativecommons.org/licenses/by-nc-nd/4.0/>).

Nomenclature			
<i>Parameter</i>		<i>cold</i>	cold stream
$T$	Temperature [°C]	<i>wf</i>	working fluid
$P$	Pressure [bar]	<i>ref</i>	reference
$\dot{Q}$	Heat flow [kW]	<i>is</i>	isentropic
$\dot{W}$	Work [kW]	<i>th</i>	thermal, first law
$\dot{M}$	Mass flow [kg/s]	<i>exg</i>	exergetic, second law
$\eta$	Efficiency	0	dead state
$\dot{X}$	Exergy [kW]	<i>i</i>	i-th
$\dot{i}$	Exergy destruction rate [kW]	<i>tot</i>	total
<i>EDF</i>	Exergy destruction factor	<i>Superscript</i>	
<i>VFR</i>	Volumetric flow ratio	<i>CI</i>	Capital Investment
<i>SP</i>	Size parameter [m]	<i>OM</i>	Operation and Maintenance
<i>BWR</i>	Back work ratio	<i>Abbreviations</i>	
<i>i</i>	Rate of return [%]	<i>TLC</i>	Trilateral cycle
<i>NPV</i>	Net present value [MUSD]	<i>ORC</i>	Organic Rankine Cycle
<i>PB</i>	Payback time [y]	<i>R-ORC</i>	Organic Rankine Cycle with one IHE
<i>TCC</i>	Total capital cost [MUSD]	<i>RR-ORC</i>	Organic Rankine Cycle with two IHE
$\dot{C}$	Cost rate	<i>KC</i>	Kalina cycle
<i>EF</i>	Emissions factor [tonnesCO <sub>2</sub> /MWh]	<i>EXP</i>	expander
<i>Em</i>	Emissions saved[tonnesCO <sub>2</sub> /y]	<i>PUMP</i>	pump
$\dot{Z}$	Cost rate of capital or investment costs	<i>COND</i>	condenser
<i>N</i>	Normalised	<i>EVAP</i>	evaporator
<i>SIC</i>	Specific investment cost	<i>IHE</i>	Internal Heat Exchanger
<i>Subscript</i>		<i>MUSD</i>	Million dollars
<i>exp</i>	expander	<i>RMAD</i>	Relative mean absolute difference
<i>pump</i>	pump	<i>%CV(RMSD)</i>	Coefficient of variation of the root mean square difference
<i>cond</i>	condenser	<i>WHR</i>	Waste heat recovery
<i>evap</i>	evaporator	<i>EDF</i>	Exergy destruction factor
<i>in</i>	entering	<i>VFR</i>	Volumetric flow ratio
<i>out</i>	exiting	<i>SP</i>	Size parameter [m]
<i>cw</i>	cold water	<i>BWR</i>	Back work ratio
<i>hs</i>	heat source	<i>NPV</i>	Net present value [MUSD]
<i>hot</i>	hot stream	<i>PB</i>	Payback time [y]
		<i>TCC</i>	Total capital cost [MUSD]

of cement production corresponds to its manufacture, where drying and clinkerisation are the processes that use the most thermal energy, which is around 90% of the total spent [4]. Then, to enhance the energy efficiency, technology improvements have been used, i.e., investing in new kiln designs, widening the fuels portfolio, and introducing waste heat recovery systems [5]. Concerning these technologies, it is possible to highlight the direct use of heat in drying or pre-heating operations or indirectly for power generation.

The European Parliament policies for promoting the efficient use of energy have aims for the year 2030 of a reduction of at least 40% in GHGs compared to 1990 levels, a 32% increase in the share of renewable energies in the energy market and a 32.5% improvement in energy efficiency, among others [6]. As shown in Fig. 1, mitigation strategies for GHGs should be focused, in order of priority, on *Fuel emissions*, *Process emissions*, *Electrical energy-related emissions*, *Emissions avoidance and reduction*, and *Management mitigation measures*. *Fuel emissions* and *Process emissions* are categorised as cause group factors, while the remaining ones can be classified into the effect group factors. Factors in the cause group exhibit a direct influence on the others and are made a priority. Regarding the *Fuel emissions*, factors as pre-heater cyclone utilisation, kiln system optimisation and efficient clinker cooling, among others, are studied to reduce waste heat during cement production.

The study presented in [7] shows that the amount of waste heat potential estimated in different industrial sectors of the European Union countries rose to 300 TWh/year. Of these, a third refers to temperatures

below 200 °C (*Low quality*), 25% associated with the range between 200 °C and 500 °C (*Medium quality*) and the remaining with temperatures above 500 °C (*High quality*), largely concentrated in the steel and cement industries. The heat source quality level defines different Waste Heat Recovery (WHR) technologies or power cycle configurations. Thermo-electric generators (TEG) rely on the Seebeck effect to produce electricity from a temperature gradient with no moving parts [8], therefore, keeping maintenance costs very low and prolonging the useful life [9]. However, this technology requires heat sources with temperatures above 500 °C so that the specific cost of generated electricity is comparable with other recovery technologies such as Organic Rankine cycles (ORC) [10].

ORC constitutes a relatively mature technology for the use of waste heat at the source temperatures in the range of 150–300 °C [11]. Such a temperature range is typical for exhaust gases in various works, as in [12] where the exhaust gases from a Heavy-Duty Diesel (HDD) engine come out at temperatures of 330–509 °C and in [13] the exhaust gases also from a diesel engine come out 317–572 °C and both are coupled to an ORC cycle for waste heat recovery. In [14] the feasibility of implementing a WHR system to recover heat by radiation from the surface of the outer wall of a rotary kiln for cement that reaches temperatures of 375 °C was evaluated using a concentric aluminium absorber panel around the kiln, which is used as a heat input of recuperated ORC. Three ORC configurations are evaluated and compared in [15]; a simple ORC, regenerative ORC and ORC with an intermediate heat exchanger (IHE).

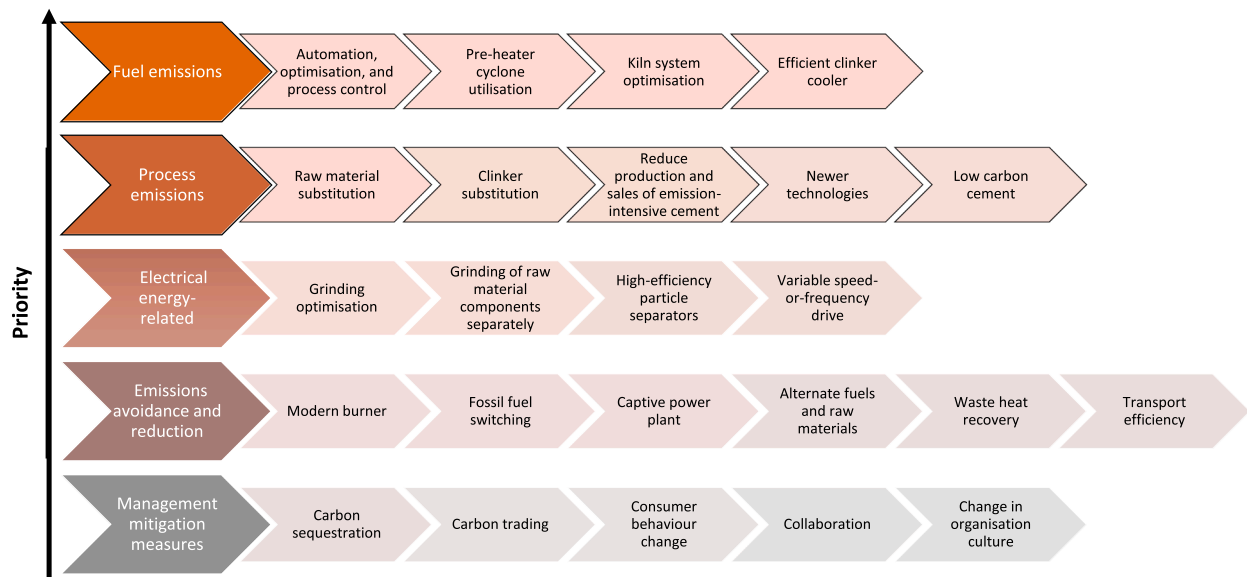


Fig. 1. GHGs mitigation strategies for cement production. Fuel emissions and Process emissions are categorised as cause group factors, while the remaining factors are in the effect group factors. Adapted from [1].

The ORC with the IHE exhibited approximately 0.4–5% and 2.53–8.78% more net power output compared to the regenerative ORC and the basic ORC, respectively. The authors [16] focus their research on choosing the architecture of an ORC cycle that uses two heat sources at different temperatures (573–773 K) and (353–393 K) to achieve better performance. The architectures analyzed were a serial two-stage ORC (STORC) and a parallel two-stage ORC (PTORC) and compared them with a single-stage preheated ORC under subcritical conditions. STORC had the highest thermodynamic performance in the investigated temperature range. With an 8.3% increase in power compared to the preheated ORC and a 27.9% reduction in the size of the heat exchanger. As for PTORC, it presented a negative performance compared to the preheated ORC, as it had a decrease in power of 0.3%.

Another WHR option is the Kalina cycle (KC), which, unlike ORC and TLC, uses a mixture of ammonia and water as the working fluid. This type of mixture is known as non-azeotropic; it has variable phase change temperatures at constant pressure, which implies an excellent thermal performance between the hot and cold streams [17]. This behaviour during the phase change allows the reduction of irreversibilities since the temperature profile between the working fluid and the heat source are more closely matched than in an ORC. The KC cycle has better thermodynamic performance than an ORC evaluated under the same heat source conditions, with a 10–20% improvement in thermal efficiency [18]. But this advantage is more pronounced when the cycle works with a sensible heat source that is between 300–600 °C, and there is a large temperature drop [19]. However, as the ammonia-water mixture has lower boiling temperatures than the working fluids used in a conventional ORC, the KC cycle can operate at even lower temperatures (100 °C) [20]. On the other hand, to obtain these yields, KC requires operating pressures up to 10 times higher than an ORC under the same heat source conditions [21]. Another important aspect is that the cost of implementing a KC is usually higher than that of an ORC [22]. A theoretical study conducted in [17] presents power generation integration with a cooling application combining two sub-cycles based on the ammonia-water mixture as a working fluid. The first corresponds to a KC variation with a net power output of 647 kW, while the second is an absorption cooling system. It is found that the total energy efficiency and the cooling to power ratios of the developed system increased by the maximum values of 6.6% and 100%, respectively, in comparison with the separated systems. In [23] the authors carried out a comparative study of two Kalina cycle configurations, KCS1, and KCS34 that used the

exhaust gases of the cyclone preheater as a waste heat source for the generation of electricity. The cycles are modelled in the Engineering Equations Solver software and optimised employing a genetic algorithm with net work and total capital cost as objective functions. In terms of total capital cost and delivered net power, up to 3.3 MW, the KSC1 is more competitive for larger capacities in daily cement production, more than 5000 tonnes/d with medium–high temperature heat source. In comparison, the KCS34 cycle turned out to be more attractive for smaller capacities and lower temperature heat sources.

Alternatively to ORC and KC, low-grade heat sources could be better accessed through the trilateral flash cycle, also known as trilateral Rankine cycle, often referred to as TFC or TLC. [24]. Such a power cycle is equivalent to a modified ORC in which the organic working fluid is heated until the saturation temperature. Instead of expanding from saturated or superheated steam like in a conventional ORC, the expansion stage begins from the saturated liquid zone, therefore, generating two phases in the fluid during the entire expansion process [25]. Comparative analytical studies have been conducted that conclude that TLC delivers approximately 50% more power than a conventional ORC working under the same heat source conditions with a temperature below 100 °C. TLC even can generate power from heat sources below 80 °C where an ORC is not economically viable [26]. However, among the negative aspects, such a power cycle usually requires higher pump power and larger heat exchangers that increase the capital costs, although it can be outweighed by the additional gain in net power [27]. The TLC's main drawback is the need for a sophisticated expander that could adequately handle the liquid phase's presence during the expansion, which ultimately discards the use of turbo-expanders due to the damage caused by the drops of liquid that hit the rotor blades [28]. Twin-screw expanders consist of helical rotors with a clearance of around 50 μm, medium friction, low leakage losses, medium noise, and a relatively high cost. These expanders seem to be the most suitable technology since they could operate smoothly with high flow rates of the working fluid, and thanks to their positive displacement nature and the ability to operate at high rotational speeds, they do not present notable decreases in their efficiency [29]. However, this type of two-phase expanders is not mature enough; therefore, it is not commercially available, posing a delay in the widening of the implementation of this system [30]. In [26] an experimental study of a system based on a TLC cycle with a net power output of 43 kW is carried out. It operates with a Pelton turbine with a stationary nozzle configuration as an expander. The

system showed promising generation capacity even with heat source temperatures below 80 °C, considering the large sizes of the heat exchangers and the pump. The study showed that for these systems, the power generation potential depends significantly on the expander nozzle's isentropic efficiency. In [31] the authors perform a simulation of a TLC with a twin-screw expander with an isentropic efficiency of 74%. Under reference conditions of the hot source (mass flow of 7.84 kg/s and inlet temperature of 85 °C) an optimal net power of 103 kW and a thermal efficiency for TLC of 6.4% were achieved. Regarding the economic analysis for the generation of TLC power cycle at a commercial scale, it has been stated that the payback time would be 8.9 years with a specific cost of the plant of 6.4 USD/W, which is undoubtedly promising even with a thermal efficiency of 1% [26].

A thorough comparison between KC and ORC is presented in [21], exhaust gases at 346 °C are used as waste heat source for the power cycles, achieving 1615 kW and 1603 kW respectively. However, the KC utilisation is disadvantageous. The performance gain does not match the additional complexity of the larger surface in the heat exchanger and the need for materials resistant to high pressures (100 bar against about 10 bar for the ORC cycle) and corrosion. A comparative performance study of an ORC, TLC, and a KC with a low-grade heat source (120°) are carried out in [32]. Three different ammonia-water mixtures for the KC and seven working fluids for the ORC and TLC are evaluated from an economic perspective. The ammonia-water mixture with 90% ammonia obtained the best performance. In the case of the ORC and TLC, the working fluid with the best performance was n-butane. With these heat source conditions, the authors state that the TLC power system can only be viable if the expander has an isentropic efficiency close to conventional turbines, around 85%. However, the isentropic efficiency of the expanders used for TLC is usually less than 70% [33], these authors carry out a broad theoretical, experimental study on TLC and twin screw expanders confirming these efficiencies. In [27] the authors compare a TLC using water as the working fluid against four ORC configurations. It is found that the TLC outlet expander volumetric flow is between 2.8 and 70 times greater than at the inlet. For this reason, they recommend working fluids such as Cyclo-Pentane, n-pentane, or n-butane that exhibit higher vapour pressures.

To summarize, among the three technologies, the ORC and KC are quite mature technologies that, for years, have proven to be very valuable as systems for converting sensible heat into mechanical energy [21]. These cycles are very efficient alternatives to generate energy from low and medium temperature heat sources. The ORC has a significant advantage over the Kalina cycle, and it is its incredible simplicity gives it reliability, flexibility, and ease of maintenance. On the other hand, the KC can be a more complex cycle due to a large number of components, but it can have a better performance from the point of view of the second law [34]. On the other side, the TLC is a technology that is still in technical development and is less well known. However, this cycle has attracted significant interest in recent years as it provides a better match between temperature profiles in the evaporator than conventional heat recovery cycles. This has the particularity that the working fluid at the inlet of the expander is in a saturated liquid state, which implies the presence of two phases during expansion. The TLC shares the simplicity of the ORC since the components of the system are the same except for the expander, since due to the expansion in two phases, it must be positive displacement, usually a screw expander [32].

After an exhaustive review of the related literature, it is determined that there is a lack of information on the thermodynamic behaviour of TLC waste heat recovery systems. Especially from the perspective of the exergue-economy analysis. Regarding simultaneous comparisons of TLC with other technologies such as ORCs and Kalina cycles, it is found that the information gap is even more significant. In this sense, this work aims to help reduce this information gap and provide results that help understand this technology better. Additionally, this work has a simple environmental approach where the potential for reducing emissions due to electricity generation is shown for each of the evaluated technologies.

On the other hand, this work was developed within the framework of a university - industry agreement. This type of relations allows the transfer of knowledge and technology between the parts, which can result in economic development and therefore an increase in competitiveness.

The authors of the present work performed a preliminary study that assessed a waste heat source constituted by hot effluent gases at 327 °C from the rotary kiln of a cement production facility with a capacity of 5000 tonnes per day [35]. Such gases contain particulate matter that is removed in a bag filter before going out of the process that operates at 180 °C to prevent thermal deterioration. Therefore, water injection is used to cool down the stream in a pre-conditioning tower, incurring thermal losses of the order of 32 MW. Such available energy was the input for comparing the thermal, exergetic, and economic performance of two WHR strategies: a drying unit and an ORC. As the main result of that study, a recuperated ORC using Cyclo-Pentane as working fluid and a heat source outlet temperature of 180 °C was the best, delivering a net power of 4.1 MW and an NPV of 0.42 MUSD. However, such work falls short in exploring alternatives regarding the power generation cycle configuration, more variety of working fluids and operating conditions, among others. Consequently, this work addresses a simulation-based analysis to evaluate the performance and WHR potential of a Kalina cycle (GC-KCI) and a simple TLC (GC-TLC) against other ORC set-ups. In the current process of the plant, the combustion gases leave the furnace at a temperature of 327 °C. These gases receive treatment before being released into the environment; first, they are cooled in a cooling tower to 180 °C and pass through a bag filter to be released. Therefore, the temperature of 180 °C and below and above this in intervals of 30 °C (120, 150, 180 and 210 °C) were selected as the exit temperatures of the cycles. In contrast, the inlet temperature of the heat source to the cycles remains unchanged at 327 °C, which is calculated taking into account heat losses due to convection and radiation in the pre-conditioning tower. Subsequently, potential savings of CO<sub>2</sub> emissions are estimated for each technology, considering an emission factor of Colombia's interconnected national system. Energy, exergy and cost calculations are assisted respectively with Aspen Plus V.10 and Aspen Process Economic Analyzer (APEA) software. Section 1 describes the methodology followed to perform the exergo-economic analysis and corresponding validations of the models used. Then, Section 3 presents significant results in terms of the thermodynamic and exergo-economic performance of the evaluated power cycles. Finally, conclusions are provided in Section 4.

## Materials and methods

Following the results of our previous work [35], power generation constitutes the most appropriate strategy, in terms of energy, exergy and costs, to access the waste heat from the hot gas effluent of the rotary kiln in a cement production facility. However, only simple ORC and with a recuperator (R-ORC) set-ups were evaluated. Then, it is significant to know the potential effect of the type of power cycle on the performance of a waste heat recovery strategy for power generation. Therefore, this section presents a description of the power cycles evaluated, characteristics of the working fluids selected, thermodynamic models used for each component regarding the exergo-economic analysis and the corresponding validations of the models used.

### Waste heat recovery power cycles

In this work, three families of power cycles will be evaluated and compared, namely ORC, TLC, and Kalina, using different working fluids and operating conditions, looking for the best performing scenario to recover waste heat. The ORC and Kalina also include intermediate heat exchangers to use the available energy better if possible, usually seen in higher delivered net work. Some parameters are fixed to carry out the comparison of the cycles:

1. The entry temperature of the heat source will remain constant at 327 °C;
2. The condenser (COND) operates with cooling water, entering at ambient temperature;
3. The working fluid outlet temperature from the condenser is held at 60 °C; and,
4. All pressure drops in the cycle occur in the expander.

The remaining conditions are treated in detail for each cycle but keeping up with the requirement of maximum delivered net work. In this section, the sketch, mathematical modelling and details of each cycle are presented. Table 1 summarises the main characteristics, advantages and disadvantages of the evaluated cycles and brings some context for further discussion.

*Organic Rankine Cycle and Trilateral flash cycle*

Schematically the TLC and basic ORC cycles are identical as shown in Fig. 2a, with just four main components: Evaporator, Expander, Condenser, and Pump. However, in practice, they differ significantly in that the TLC expands the working fluid directly from the saturated liquid area, generating two phases during the expansion process [25]. Fig. 2b shows the T–s diagram of the configuration for the TLC and simple ORC cycles, where this is readily appreciated. Although posing additional requirements for real-world applications, the two-phase expansion is modelled precisely like its more common non-condensing counterpart. However, such expanders at a lower maturity are usually more expensive and less efficient, which must be considered for the comparison.

The scheme outlined in Fig. 2a serves as a basis for more complex configurations of the ORC, that is, adding intermediate heat exchangers. In the case of a single exchanger, R-ORC, the low-pressure steam flow in the stream (4) is used to preheat the feed to the evaporator (2). Thus, a single intermediate heat exchanger benefited the performance of the basic cycle and was applied satisfactorily previously [35]. However, it is still possible for the heat source analysed to include a second intermediate heat exchanger, RR-ORC, as shown in Fig. 3a; here, the low-

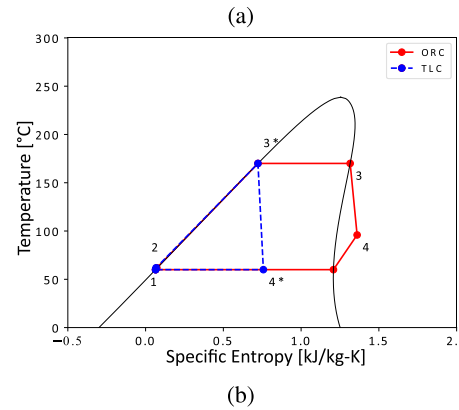
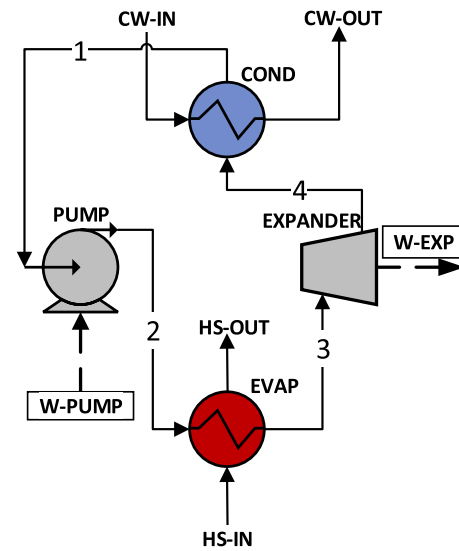


Fig. 2. Organic and Trilateral flash cycle configuration (a) and T–s diagram (b).

Table 1  
Cycles characteristics, advantages and disadvantages.

	ORC	TLC	KC
Working fluid	Alkanes and refrigerants.	Alkanes and refrigerants.	Ammonia-Water mixture.
T [°C]	150–300 [11].	80–200 [36].	100–600 [19,20].
P [bar]	Up to 45 [36].	Up to 45 [36].	Up to 10 times more than an ORC for the same heat source conditions [21].
Cost/ $\dot{W}_{net}$	Medium	High	High
Advantages	<ul style="list-style-type: none"> <li>• Low operating pressures.</li> <li>• Few components.</li> <li>• Does not require overheating if dry or isentropic fluids are used.</li> </ul>	<ul style="list-style-type: none"> <li>• Low operating pressures.</li> <li>• Few components.</li> <li>• It can operate with very low temperature sources (80 °C), and delivers more net work than an ORC at low temperatures.</li> </ul>	<ul style="list-style-type: none"> <li>• More efficient than a conventional ORC.</li> <li>• It has a wide operating range in terms of heat source temperatures.</li> <li>• Due to the non-azeotropic mixing, it takes better advantage of the heat source (destroys less exergy).</li> </ul>
Disadvantages	<ul style="list-style-type: none"> <li>• Difficulty operating with low temperature sources &lt;100 °C.</li> </ul>	<ul style="list-style-type: none"> <li>• It cannot exceed the critical temperature of the working fluid.</li> <li>• Low expander efficiency and high cost.</li> </ul>	<ul style="list-style-type: none"> <li>• It has many components.</li> <li>• High cost.</li> <li>• High operating pressures.</li> </ul>

pressure steam flow coming out of the expander is used to preheat the stream (2) entering the evaporator. However, such a stream is heated further using the exhausted combustion gases of the source once they leave the evaporator. Such a modification has two main objectives: to use as much heat as possible from the waste heat source, removing the gases at the lowest possible temperature, ensuring non-condensation, and to increase the evaporator temperature to achieve higher thermodynamic efficiency in the cycle.

*Kalina cycle*

The Kalina cycle’s peculiarity relies on its working fluid; the ammonia-water mixture forms a zeotrope, which allows having a range of temperatures for evaporation and condensation in contrast to pure substances, where phase changes occur at a single point [37]. This variability in evaporation and condensation temperatures facilitates a better thermal match between the heat source and the working fluid temperature profiles, that is, reducing irreversibilities during heat transfer which can be understood as less exergy destruction [38].

The Kalina cycle configuration explored in this work is illustrated in Fig. 4a. It corresponds to a modification proposed in [39] of the basic cycle, which is applicable for waste heat recovery in the cement industry; such a set-up is especially suitable for higher source temperatures. The primary heat input to the cycle occurs in the evaporator (EVAP). This is in charge of heating the stream (2-2), which is composed of a mixture of ammonia-water that is not fully evaporated (3-1) and must be taken to a separator (SEP) which divides the stream into two: an ammonia-rich vapour stream (3-2) and an ammonia-poor liquid stream

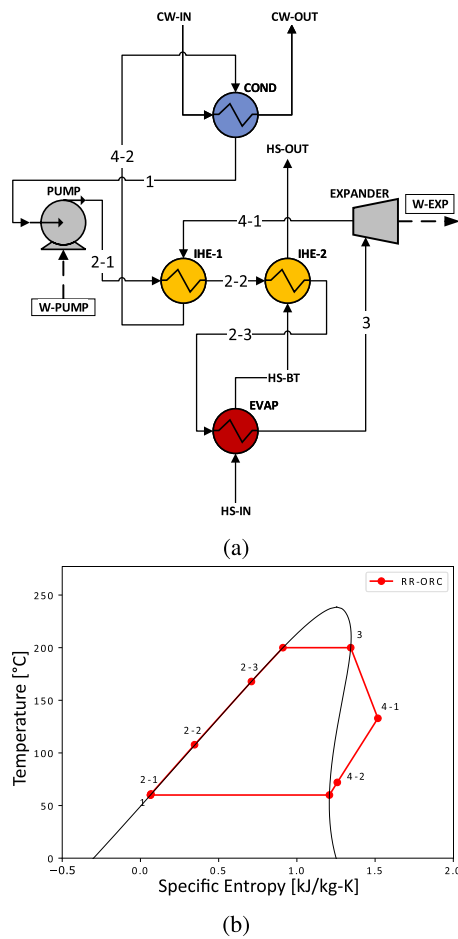


Fig. 3. Recuperated Organic cycle configuration (a) and  $T-s$  diagram (b).

(3-4). Then the vapour stream is superheated in an intermediate heat exchanger (IHE-2) with the heat source inlet (HS-IN). The superheated stream (3-3) is then passed to an expander, where mechanical power is generated. The liquid stream coming from the separator is expanded through a valve that takes it to the expander discharge pressure; these two streams are mixed, resulting in the stream (4-3), which is taken to a low-temperature heat recovery unit (IHE-1). Finally, the low-pressure liquid stream is passed through a pump and pressurised to the evaporation pressure. Thus, stream (2-1) is in charge of recovering the heat in IHE-1 and closing the cycle in the evaporator.

Some cycle variables that could interfere are set to analyse the effects of the change in the concentration of the ammonia-water mixture and the outlet temperature of the heat source gases. First, the isentropic efficiency for the turbine found in the literature usually vary from 75–85% and the isentropic efficiency of the pumps from 60–70% [21,40,41]. However, for this work, both are set to be 75%. Second, stream (2-2) enters the evaporator as a saturated liquid. Third, the evaporator pinch point is set at 32.5 °C, while a minimum pinch temperature of 10 °C is defined for the IHE-2 exchanger considering that this temperature usually varies in the range of 5–20 °C according to [42–44]. For convergence and to facilitate the Kalina cycle study at different concentrations of the ammonia-water mixture, the pinch point temperature in the IHE-1 exchanger is not fixed yet tuned for each case. When considering the heat source outlet temperature of 210 °C, the evaporator pinch point temperature is set to be 62.6 °C to avoid a temperature crossover in the IHE-1 heat exchanger.

*Working fluid selection for Organic Rankine Cycle and Trilateral flash cycle*  
The selection of the appropriate working fluid is a fundamental step

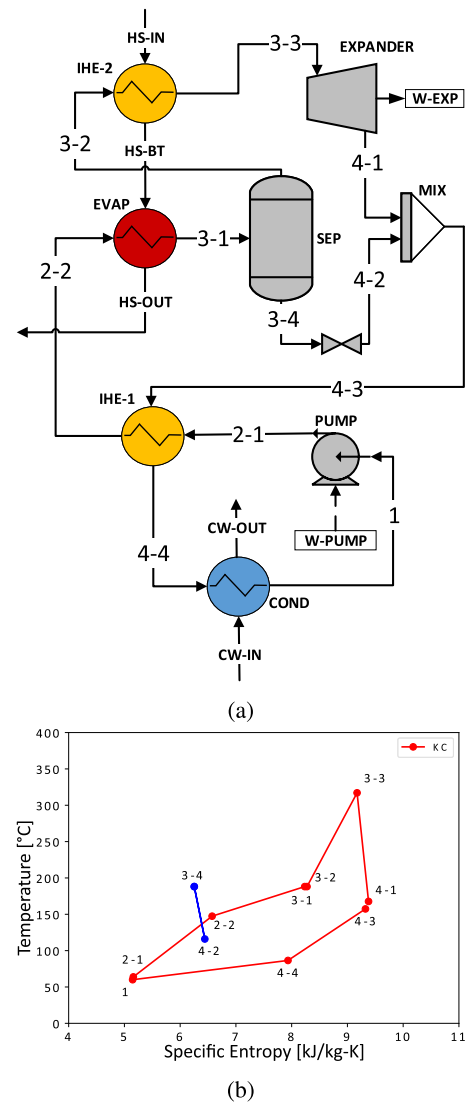


Fig. 4. Kalina cycle configuration (a) and  $T-s$  diagram (b).

when defining a power cycle since it conditions the performance, safety, and environmental responsibility of its operation. Therefore, it makes sense to explore the advantages and disadvantages of some of the more common alternatives. For example, in ORC and TLC, it is usual to use pure organic fluids such as refrigerants and alkanes, the former being generally safer. However, one working fluid's energy, exergy and economic performance are closely linked to its operating conditions, the alkanes being more suitable when operating temperatures are higher [45]. Regarding the modelling of the thermodynamic properties of these fluids, it is common to use cubic equations of state. In the case of this work, Peng-Rob (PR) is used for the gas phase. Regarding working fluids for trilateral cycles, better performance could be achieved when the working fluid's critical temperature approaches the temperature of the heat source [46]. Moreover, it must be selected considering the reduction in the volumetric flow ratio in the expander, which is related to its size and cost, potentially impeding its practical application if it is too large [47]. Therefore, the selection of a working fluid with a low volumetric flow ratio in the expander is necessary to promote the development of TLCs.

In [48] it is shown that the influence of parameters such as the critical temperature and the heat capacity of the working fluid in the TLC's performance to define the most suitable for the two-phase expansion. The authors evaluated fifteen theoretical working fluids

spanning five critical temperatures (100, 125, 150, 175, and 200 °C) and four heat source temperatures (80, 120, 160, and 200 °C). These fluids are selected within a design space occupied by existing working fluids. Under these conditions, they optimise the net power output of the system for each of the heat source temperatures. Subsequently, it was possible to identify seven real working fluids with critical temperatures ranging between 132.8 °C (isobutane) and 196.7 °C (n-pentane). The optimisation procedure for these fluids was carried out for heat source temperatures of 80, 120, 160, and 200 °C; the optimal working fluids were R245ca, isopentane, n-butane, and n-butane, respectively. When a working fluid is selected for a TLC, it is done from the point of view of the expander [46], seeking to reduce the volumetric flow ratio, VFR, between its inlet and outlet.

In [49], it is shown that single-stage power cycles, are only possible with VFR values < 50. Therefore, in this work, all configurations that had a VFR outside of this limit were discarded. Eight working fluids of the 57 reported by [36] are analysed, with critical temperatures between 170 and 200 °C. Then, they are simulated under three temperature settings at the exhaust gas outlet (120, 150, 180 °C). For the TLC configuration, the cycle with an outlet temperature of 210 °C was not evaluated because, under this condition, the temperature of the working fluids at the inlet of the expander exceeds the critical temperature of all fluids. Therefore, at this point, the working fluid is in the gaseous state, which is not supported in a TLC configuration. The inlet temperature of the exhaust gases to the heat exchanger remained unchanged in all configurations and was 327 °C.

**Thermodynamic model**

The thermodynamic modelling of all power cycles relies on the straightforward application of mass, energy, and exergy balances. These are listed in Table 2: Eq. (2) presents the calculation of the exergy for any stream in the cycle. The equations in the first-law column account for: the heat that enters the cycle in the evaporator, Eq. (2), the heat that leaves the cycle in the condenser, Eq. (2), the work delivered by the expander, considering its mechanical and isentropic efficiencies, Eq. (2), the work required by the pump according to its isentropic efficiency, Eq. (2). In the case of the column of second-law equations, the exergies destroyed by each of the components involved in the cycle, it is defined according to: Eq. (2) evaporator, Eq. (2) condenser, Eq. (2) expander, Eq.

(2) pump. Finally, the calculation of the heat transferred by the intermediate heat exchangers, if present, appears in Eq. (2) and the exergy destroyed by them, in Eq. (2).

The information in this table is insufficient to determine the individual performance of each of these power cycles. Therefore, it must be complemented with Table 3, which presents the equations that describe the most used performance indicators:

- T power cycle's net work is calculated in terms of the work of the expander and the pump in Eq. (3);
- 1st-law efficiency depends on the net work and the heat input to the cycle, Eq. (3);
- Exergy efficiency is calculated in terms of the useful exergy (delivered net work) and the exergy input to the cycle, Eq. (3);
- The total destroyed exergy by the cycle is estimated as the sum of the destroyed exergy of each component of the cycle, Eq. (3);
- The exergy destruction factor EDF is an indicator that relates the total destroyed exergy by the cycle to the delivered net work; therefore, the EDF is higher if the destroyed exergy is greater;
- The volumetric flow ratio, Eq. (3), gives an idea of the volume change of the working fluid in the expander; thus, if this exceeds the value of 50, several stages of expansion must be considered. [50]. Then, the lower the VFR, the better;
- The size parameter of the expander, Eq. (3), is used to estimate the approximate diameter of the required expander, and it is linked to its actual size and cost. The lower the SP, the smaller and cheaper the expander [51];
- The back-work ratio of the cycle is useful to grasp an idea of the size and energy requirements of the pump, it is calculated as the ratio of the pump and the expander work, Eq. (3), and it is higher for those alternatives that require larger pumps.
- The cycle normalised net work Eq. (3), is a measure of the delivered net work per mass flow of working fluid. Such an indicator could be easily linked to costs and safety of the working fluid and space and weight requirements in the case of off-shore or marine applications [52].
- Specific investment cost (SIC) Eq. (3), is a common indicator used in preliminary economic assessments of Power cycles. This metric represents the total capital cost (TCC) of the system per rated kW of generated power.[53].

**Table 2**  
Energy and exergy balance equations.

Component	1st-law equations	2nd-law equations
ith-stream	-	$\dot{X}_i = \dot{m}_i [(h_i - h_0) - T_0 (s_i - s_0)]$ (1)
Evaporator	$\dot{Q}_{in} = \dot{m}_{hs} (h_{hs,in} - h_{hs,out})$ (2)	$\dot{I}_{evap} = (\dot{X}_{hs,in} - \dot{X}_{hs,out}) - (\dot{X}_{out} - \dot{X}_{in})$ (3)
Condenser	$\dot{Q}_{out} = \dot{m}_{cw} (h_{cw,out} - h_{cw,in})$ (4)	$\dot{I}_{cond} = (\dot{X}_{in} - \dot{X}_{out}) - (\dot{X}_{cw,out} - \dot{X}_{cw,in})$ (5)
Expander	$\dot{W}_{exp} = \dot{m}_{wf} (h_{in} - h_{out,s}) \eta_{is,exp} \eta_{mech,exp}$ (6)	$\dot{I}_{exp} = (\dot{X}_{in} - \dot{X}_{out}) - \dot{W}_{exp}$ (7)
Pump	$\dot{W}_{pump} = \dot{m}_{wf} (h_{out,s} - h_{in}) / \eta_{is,pump}$ (8)	$\dot{I}_{pump} = (\dot{X}_{in} - \dot{X}_{out}) + \dot{W}_{pump}$ (9)
IHE	$\dot{Q}_{IHE} = \dot{m}_{wf} (h_{hot,in} - h_{hot,out})$ (10)	$\dot{I}_{IHE} = (\dot{X}_{hot,in} - \dot{X}_{hot,out}) - (\dot{X}_{cold,out} - \dot{X}_{cold,in})$ (11)

**Table 3**  
Performance indicators.

Performance Indicator	Equation
Net work	$\dot{W}_{net} = \dot{W}_{exp} - \dot{W}_{pump}$ (12)
1st-law efficiency	$\eta_{th} = \frac{\dot{W}_{net}}{\dot{Q}_{in}}$ (13)
2nd-law efficiency	$\eta_{exg} = \frac{\dot{W}_{net}}{\dot{X}_{hs,in} - \dot{X}_{hs,out}}$ (14)
Total destroyed exergy	$\dot{i}_{tot} = \sum_i \dot{i}_i$ (15)
Exergy destruction factor	$EDF = \frac{\dot{i}_{tot}}{\dot{W}_{net}}$ (16)
Volumetric flow ratio	$VFR = \frac{\dot{V}_4}{\dot{V}_3}$ (17)
Size parameter	$SP = \frac{\sqrt{\dot{V}_4}}{(h_3 - h_{4s})^{1/4}}$ (18)
Back work ratio	$BWR = \frac{\dot{W}_{pump}}{\dot{W}_{exp}}$ (19)
Normalised net work	$N\dot{W}_{net} = \frac{\dot{W}_{net}}{\dot{m}_{wf}}$ (20)
Specific investment cost	$SIC = \frac{TCC}{\dot{W}_{net}}$ (21)

**Parameters and boundary conditions**

The parameters and boundary conditions for each of the cycle configurations in this work and the ones used for same heat source in [35] are summarised in Table 4. The case studies are analysed by varying the temperature of the heat source when exiting the waste heat recovery or power cycle alternative. Thus, in ORCs, the gases pass through the

**Table 4**  
Parameters and boundary conditions for all cycle configurations.

Stream	Units	ORC	ORC + DRYER	R-ORC	TLC	KC	RR-ORC
HS-IN	°C	327	327	327	327	327	327
HS-OUT	°C	120 150 180 210	180	180	120 150 180	120 150 180 210	120
3	°C	110 140 170 200	170	170	110 140 170	110 140 170 200	170 200
1	°C	60	60	60	60	60	60
CW-IN	°C	27.8	27.8	27.8	27.8	27.8	27.8
CW-OUT	°C	37.8	37.8	37.8	37.8	37.8	37.8
$\eta_{is,pump}$		0.7	0.7	0.7	0.7	0.75	0.7
$\eta_{is,exp}$		0.85	0.85	0.85	0.7	0.75	0.85

evaporator and exit at 210, 180, 150 or 120 °C. On the other hand, in the TLC, an outlet temperature of 210 °C is discarded as it is impossible to expand from saturated liquid at this temperature using the selected working fluids. Table 5 shows the selected working fluids for ORC and TLC, with their critical properties.

In the case of KC, outlet temperatures are the exact ones used for simple ORCs. However, due to the presence of IHES, it is necessary to modify some of the intermediate currents to meet the requirement of maximum delivered net work. This parameter conditions the performance of a heat recovery alternative from the thermodynamic analysis and the costs since this is considered the valuable exergy current. Therefore, for ORCs with IHES and combined with the drying unit from previous work [35], only best candidates are explored, that is, those with highest delivered net work and positive net present value, NPV.

**Exergo-economic analysis cost models**

The traditional specific exergy cost method (SPECOC) outlined by [54] is followed to thoroughly compare the alternatives considered for WHR in the cement plant as it considers the interactions between exergy and average unit costs of the streams. It has been successfully applied in similar works. In [55] the authors carry out an exergo-economic study using the specific exergy cost method (SPECOC) on a two-stage organic Rankine cycle (ORC) combined with a heat pump cycle (ORC-HP), that uses the heat generated from the combustion of solid urban solid waste with a lower heating value (LHV) of 10.5 MJ/kg, in which the investment recovery time is used as a decision criterion, which for the case was 0.48 years. In [56] the SPECOC methodology is used to evaluate the exergo-economy of a cogeneration system that includes an absorption power cycle (APC) and a humidification-dehumidification desalination (HDH) unit, to provide the necessary energy and freshwater for the crew of a ship. Exhaust gases from a marine diesel engine (MDE) are used as a waste heat source. This system could produce 13.03 kW of power and 0.235 kg/s of fresh water. In [57] they carried out an exergo-economic study using the SPECOC methodology on two different technologies that are suitable for taking advantage of low and medium temperature geothermal energy. These technologies are Organic Rankine (ORC) and Kalina (KC) cycles. The low temperature source (120 °C) located in the Pomarance geothermal basin, Italy. The medium temperature source (212 °C) located on Mt. Amiata, Italy. In the low temperature case study, KC showed the best performance, producing between 22 and 42% more net-work than ORC. In this case, the cost of electricity produced by the KC was 12.5 €/kWh, 24–34% lower than the cost of electricity produced by the ORC for the same case. For the case of the medium temperature study, the ORC with working fluid R1233zd (E) showed the best exergo-economic performance with a cost of electricity produced of 8.85 €/kWh, which was 3% lower than that of KC.

The general cost balance equation for a system that employs a heat input to deliver net work is expressed as follows,

$$\sum \dot{C}_e + \dot{C}_w = \sum \dot{C}_i + \dot{C}_q + \dot{Z}_t \tag{22}$$

**Table 5**  
Critical properties of selected fluids for TLC and ORC.

Cycle	Working fluid	$T_{cr}$ [°C]	$P_{cr}$ [Bar]	
TLC	R11	197.96	4.41	
	R141b	204.35	4.21	
	R21	178.33	5.18	
	R365mfc	186.85	3.27	
	Isopentane	187.2	3.38	
	R123	183.68	3.66	
TLC, ORC	R245ca	174.42	3.93	
	Pentane	196.55	3.37	
	ORC	R1234yf	94.7	3.38
		R134a	101.06	4.06
		CycloPentane	238.54	4.52

where the sum of the cost rates of the exiting streams ( $C_e$ ), and net work ( $C_w$ , must be equal to the sum of the cost rate of the entering streams ( $C_i$ ), the heat input ( $C_q$ ), and the sum of the capital investment costs and the operation and maintenance costs rates ( $Z_t$ ). The latter is calculated as

$$\dot{Z}_t = \dot{Z}^{CI} + \dot{Z}^{OM} \quad (23)$$

where ( $\dot{Z}^{CI}$ ), and ( $\dot{Z}^{OM}$ ) are estimated using the APEA software and the capital recovery factor for the annualisation of the total capital costs (TCC) as thoroughly described in [35]. Some of the parameters used to estimate costs are: the cost of electricity from the grid,  $c_{el} = 0.07$  \$/kWh; the cost of cooling water,  $c_{cw} = 0.027$  \$/m<sup>3</sup>; the cost of fuel for a cement plant,  $c_{fuel} = 3.84$  \$/GJ [58]; 20 years cash flow for the plant; all the heat exchangers are treated as shell-and-tubes; the expanders as non-condensing turbines, except for the TLC, where condensing turbines are used instead; all pumps are centrifugal; the cost of the separators, mixers, and valve in the Kalina cycle is considered negligible.

Finally, the economic performance parameters chosen for this analysis are: total cost of capital (TCC), rate of return on investment (%i(return)), payback time PB, and net present value NPV, the latter being the most crucial decision criterion, since WHR alternatives with negative values are discarded.

### Validation

This section presents the cross-validation with the literature of the performed simulations. Section 2.3.1 considers the ORC/TLC, while Section 2.3.2 carefully explores the case of the Kalina cycle and the ammonia-water mixture.

#### Organic Rankine cycle/Trilateral Flash cycle

Regarding the modelling of power cycles with pure organic fluids and refrigerants, the Peng Robinson, PR, model is the most widely used in the literature. In [59], a two-dimensional non-viscous computational fluid dynamic model is applied to a typical supersonic turbine cascade for ORC applications. The working fluid is MDM siloxane, which under the conditions of interest exhibits relevant non-ideal effects. The authors modeled using a Peng-Robinson equation of state. on the other hand, in [60] the authors performed an analysis of an ORC cycle combined with a phosphoric acid fuel cell (PAFC); to recover residual heat from a fire-place. They considered 15 working fluids, mostly organic fluids and refrigerants. The thermodynamic properties of these fluids were calculated with the Peng-Robinson equation of state. Table 6 shows the parameters and results of the validation of the PR model used in this research with the data reported by [32]. The chosen parameter for model validation is the thermal efficiency of the cycle instead of the net work because the authors do not report data on the mass flow of the organic fluid. The TLC showed a relative mean absolute difference, %RMAD, of 2.77% in the thermal efficiency, while for the ORC, it is 1.12%. Such a low discrepancy with reference data for the power cycles

**Table 6**  
Validation parameters for TLC and ORC models.

Parameter/Cycle	TLC	ORC
<i>Operating conditions</i>		
Working Fluid	n-Butane	R1234yf
T3 [°C]	109	84
T1 [°C]	40	40
$n_{pump}$	0.75	0.85
$n_{urb}$	0.85	0.85
$\dot{W}_{net}$ [kW]	2034	1816
<i>Validation</i>		
$\eta_{th}$ reference [32]	0.070	0.078
$\eta_{th}$ present model	0.068	0.077
RMAD [%]	2.77%	1.12%

indicates an excellent performance of the current simulations and model when replicating results.

#### Equation of state selection for the ammonia-water mixture

Although the Kalina cycle is often used for power generation, there is no consensus yet in modelling the ammonia-water mixture. In [61] it is shown that with optimised binary interaction parameters (BIP) correlations, the Redlich-Kwong (RK) and Peng-Robinson (PR) cubic equations of state (EoS), used together with the SOF function and the Margules combining rule, provide an accurate representation of the phase equilibrium and enthalpy behaviour of these mixtures. In [62] appear energy, exergy, and economic comparison of the ORC and Kalina cycles for low-temperature (100 °C) enhanced geothermal systems in Brazil. The thermodynamic analysis was carried out using Aspen-HYSYS software and the Peng-Robinson Stryjek-Vera (PRSV) EoS to estimate the working fluid's thermodynamic properties. The Kalina cycle, operating with an 84–16% ammonia-water mass fraction, showed the best performance with 1.76 MW of delivered net power and a Levelized cost of electricity of 0.22 €/kWh. [63] developed a new integrated power generation and cooling system with the compression system, liquefaction, and cogeneration unit based on the Kalina cycle which makes use of the PR and PRSV EoS to predict the properties with high accuracy; such a new integrated structure generates 11.66 MW power and 4.502 MW cooling at the on-peak time with a 40.17% exergy efficiency. A case study is presented in [42], with a Kalina cycle in a geothermal power plant located in Wayang Windu using brine from the power plant as the heat source. For the prediction of the AW system properties, the authors use the PR model. In [64] it is shown a review of the Kalina cycle research, where the authors report the results of the work of [65] on the comparison of the behaviour of the PR equation of state versus the experimental data of the WATAM program, which deduces that the PR model is adequate to model the liquid–vapour equilibrium of the AW mixture. However, it overestimates the behaviour near the critical region. Since the SRK, PRSV, and PR models are the most widely used for predicting the properties of the water-ammonia mixture and modelling the Kalina cycle, their behaviour is analysed for this work.

The Aspen Hysys tool is used to compare the values reported in the literature and determine models' accuracy. Three Kalina cycle configurations, KCI [66], KCII [20]. KCIII [39], are compared using the coefficient of variation of the root mean square deviation, %CV(RSMD) for all stream temperatures. In contrast, the relative mean absolute difference, %RMAD, is used for the delivered net power of each cycle. These indicators can be obtained from,

$$\%RMAD = ABS\left(\frac{Y_i - Y_{ref}}{Y_{ref}}\right) \times 100 \quad (24)$$

$$\%CV(RSMD) = \frac{\sqrt{\frac{1}{n} \sum_{i=1}^n (Y_i - Y_{ref})^2}}{\bar{Y}_i} \times 100 \quad (25)$$

where  $Y_i$  is the value of the calculated variable and  $Y_{ref}$  refers to the reference value.  $n$  is the number of compared points, and  $\bar{Y}_i$  is the arithmetic average of the calculated variable. These indicators were used successfully in a waste heat recovery application to compare the absolute variation between the value of a calculated variable, like the total heat flux, and a fixed reference, and to compare a point by point temperature distribution along the surface of an absorber panel as shown in [14].

Fig. 5 shows the results of the validation of the thermodynamic model as the compiled %CV(RSMD) and %RMAD of the three chosen Kalina cycle configurations. The %CV(RSMD) of the three proposed models presents an acceptable predictive capability. On average, the temperature predictive error of the PR model is 1.76%, for the PRSV model, it is 2.01%, and for the SRK model, it is 3.01%. The most critical parameter to consider in predicting the properties of the ammonia-water mixture is its concentration. The ammonia mass fraction of KCI is 0.9, for

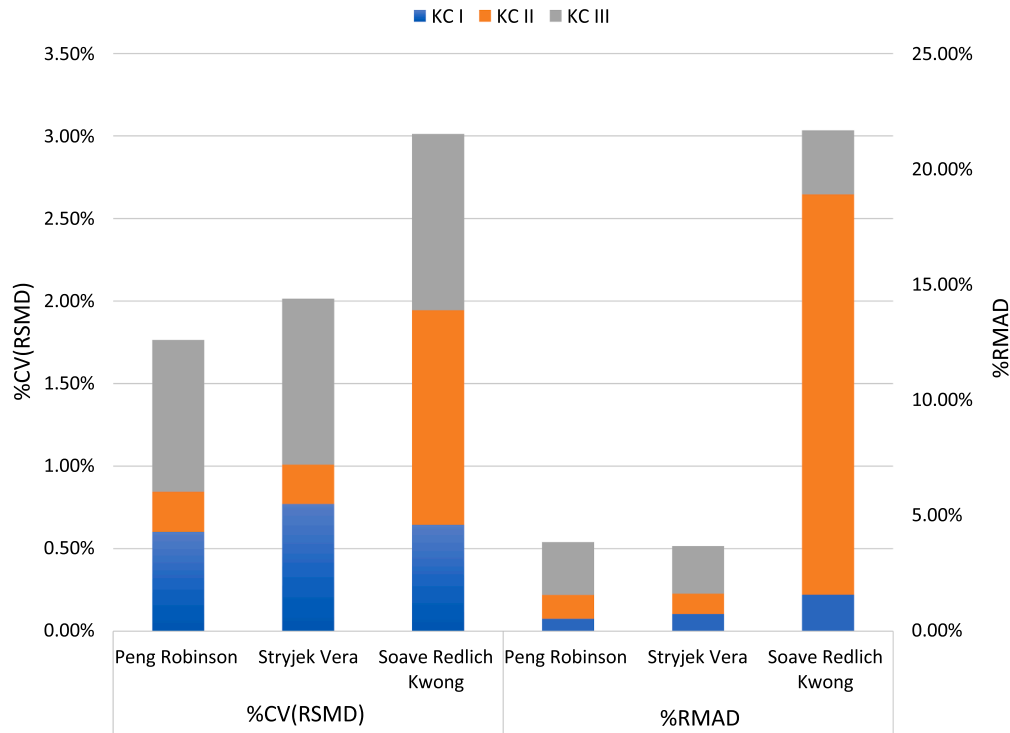


Fig. 5. Validation of thermodynamic models for the Kalina cycle.

KCII 0.95, and for KCIII 0.89. Therefore, the results of the SRK model for KCI and KCIII cycles are like the results of the PRSV and PR models. At the same time, the most significant difference is found in the KCII cycle, showing that the 95% ammonia concentration in the mixture influences the temperature prediction.

The performance of the PR model on temperature was better for KCI and KCIII configurations compared to the PRSV model. However, it is not considered a significant difference concerning the reference values. SRK model has the most significant absolute relative deviation on the net power, with the most prominent contribution being in the KCII

Table 7  
Set-up for positive NPV WHR case alternatives.

	WHR Alternative	Working fluid	HS $T_{out}$ [°C]	$\dot{Q}$ [kW]	$\dot{m}$ [kg/s]	$T_{evap}$ [°C]	$P_{evap}$ [bar]
0	ORC	Pentane	120	32990.08	76.9	110	5
1		Cyclo-Pentane			73.7		4
2		Pentane	150	28328.52	60.1	140	12
3		Cyclo-Pentane			58		8
4	ORC+Dryer	Cyclo-Pentane	150	32990.05	58	140	8
5	KC	AW-70%	150	28328.52	15.8	204.7	54.9
6		AW-75%			16.5	200.6	60.13
7		AW-80%			17.4	194.4	65.2
8		AW-85%			18.4	185.5	70.1
9	ORC	Pentane	180	23627.87	47	170	22
10		Cyclo-Pentane			45.2		16
11	ORC+Dryer	Cyclo-Pentane	180	32990.08	45.2	170	16
12	R-ORC	Cyclo-Pentane	180	23627.87	49.2	170	16
13	KC	AW-70%	180	23627.87	15.3	226.5	87.36
14		AW-75%			16	221.2	95.56
15		AW-80%			17	213.6	103.57
16		AW-85%			18.4	203	111.34
17		AW-90%			20.2	188.1	118.95
18	TLC	R11	180	23627.87	205.1	170	30
19		Isopentane			71.5		27
20		R123			168.8		30
21		R245ca			120.8		37
22	ORC	R1234yf	210	18887.17	73.4	200	33
23		R134a			67.8		40
24		Pentane			35.5		33
25		Cyclo-Pentane			34.1		26
26	KC	AW-75%	210	18887.17	12.7	221.2	95.51
27		AW-80%			13.5	213.5	103.51
28		AW-85%			14.6	202.9	111.28
29		AW-90%			16.1	188.1	118.89
30	RR-ORC	Cyclo-Pentane	120	32990.08	68.6	170	16
31			170		67.3	200	

configuration. Since the model does not predict temperature well, its influence on the net power of the cycle is observed, moving away from the reference values. The PRSV model had a lower deviation for the KCII and KCIII configurations compared to the PR model. Therefore, it predicts better the behaviour at higher ammonia concentrations. For this work, the PR model is chosen to predict the properties because it is widely used in this application. In addition, the maximum ammonia concentration is 90%, and it does not work in critical conditions. It is also recommended to use variants of the model, such as the PRSV, which exhibits an excellent predictive capacity.

**Results and discussion**

The most relevant results of the developed simulations are presented in this section and are conveniently summarised in Tables 7–10, corresponding to those WHR alternatives that exhibit positive NPV, and are relevant candidates for further consideration. The numbering of the cycles in such tables is the one to be used in Figs. 7–9. Section 3.1 presents a description of the significant results and subtleties of each kind of evaluated power cycle. Section 3.2 examines the behaviour of the exergy destroyed by components in the different cycles, while Section 3.3 presents the potential savings of CO<sub>2</sub> emissions due to implementing a WHR alternative.

*Thermodynamic and exergo-economic considerations*

This section presents the significant results in terms of the thermodynamic and exergo-economic performance of the evaluated power cycles: ORC in Section 3.1.1, TLC in Section 3.1.2, KC in Section 3.1.3.

*Organic Rankine Cycle*

The ORC stands out for its simplicity, and easy adaptability to the heat source temperature analysed 327 °C. The previous results of [35] are included in this analysis and showed that the thermodynamic and

economic performance of this type of cycle is highly dependent on the selected working fluid and the evaporation temperature. In particular, alkanes allow higher evaporation temperatures and, in turn, provide more net work, making them better candidates from an economic point of view since capital and operating costs are met quickly. However, the ORC variants that include intermediate heat exchangers favour better use of incoming heat, achieving higher efficiencies. The best performances reached in [35] were 3.77 MW of power generated by a simple ORC that operates with cyclo-pentane at an outlet temperature of the WHR system of 180 °C with a SIC of 3040 \$/kW and NPV of 0.37 MUSD. The results are conclusive with a single IHE; the delivered net work is 4.1 MW and a SIC of 1985.7 \$/kW and NPV of 0.42 MUSD for the same working fluid.

In the present work, a variant of the ORC that includes two IHEs is examined, as depicted in Fig. 3a, which allows the effluent gases from the kiln to leave the cycle at the lowest possible temperature without condensation, 120 °C, while increasing the evaporation temperature to 180 °C or 210 °C, points 30 and 31 of Table 7. These cycles fulfil the objective of increasing efficiency by taking better advantage of the heat source, extracting as much heat as possible, and in the same way, complying with the process restriction of keeping the temperature of the effluent stream below 180 °C when passing through the particle filter. Such cycles continue using cyclo-pentane as working fluid and deliver, in the best case, point 31, 6.2 MW of power with a SIC of 1718.1 \$/kW and a net present value, NPV of 0.74 MUSD. This performance far exceeds that obtained in the previous work, around 50% higher net work with 80% higher NPV, and constitutes the best alternative in terms of performance to recover waste heat from the evaluated source.

Decision-making is a process that involves more variables than just performance. Therefore, Section 3.4 will go further with the deliberation.

*Trilateral Flash Cycle*

Fig. 6 shows the volumetric flow ratio of the working fluid between

**Table 8**  
Energy and Exergy performance indicators.

	WHR Alternative	$\dot{W}_{net}$ [kW]	$\eta_{th}$ [%]	$\eta_{exg}$ [%]	$\dot{I}_{tot}$ [kW]	EDF	VFR	SP [m]	BWR	$N\dot{W}_{net}$ [kW/kg/s]
0	ORC	2129.7	6.46	16.71	10091.9	4.7	2.4	0.3	0.02	27.7
1		2590.6	7.85	20.33	9638.9	3.7	2.7	0.3	0.01	35.2
2		3297.5	11.64	28.62	7800.3	2.4	6.3	0.2	0.04	54.8
3		3481.3	12.29	30.22	7619.6	2.2	5.6	0.3	0.02	60.0
4	ORC+Dryer	3481.3	-	31.40	8743.0	-	5.6	0.3	0.02	60.0
5	KC	2271.8	8.00	17.80	9789.2	4.3	2.1	0.3	0.04	144.1
6		2598.2	9.20	22.60	8245.8	3.2	2.3	0.3	0.05	157.4
7		2936.9	10.40	25.50	7913.2	2.7	2.4	0.3	0.05	169.2
8		3302.6	11.70	28.70	7554.2	2.3	2.6	0.3	0.05	179.7
9	ORC	3347.1	14.17	33.30	6360.4	1.9	14.1	0.2	0.06	71.3
10		3770.6	15.96	37.52	5944.1	1.6	12.1	0.2	0.03	83.4
11	ORC+Dryer	3770.6	-	31.40	8410.4	-	12.1	0.2	0.03	83.4
12	R-ORC	4100.5	17.35	40.80	5619.9	1.4	12.1	0.3	0.03	83.4
13	KC	2910.4	12.30	29.00	6790.8	2.3	3.1	0.2	0.06	190.6
14		3268.5	13.80	32.50	6439.2	2.0	3.4	0.2	0.07	205.0
15		3651.6	15.50	36.30	6063.1	1.6	3.6	0.2	0.07	215.4
16		4094.7	17.30	40.70	5628.1	1.4	3.8	0.2	0.08	223.0
17		4680.2	19.80	46.60	5053.2	1.1	4.0	0.3	0.09	232.1
18	TLC	2121.6	8.98	21.11	7565.0	3.6	37.6	0.2	0.21	10.3
19		2214.6	9.37	22.03	7473.5	3.4	46.8	0.2	0.16	31.0
20		2216.2	9.38	22.05	7471.9	3.4	42.5	0.2	0.18	13.1
21		2279.3	9.65	22.68	7409.9	3.3	41.9	0.2	0.16	18.9
22	ORC	1078.9	5.71	12.91	6977.9	6.5	2.0	0.2	0.15	14.7
23		1377.8	7.29	16.48	6684.1	4.9	2.4	0.2	0.13	20.3
24		2883.0	15.26	34.49	5204.7	1.8	25.7	0.2	0.08	81.3
25		3388.7	17.94	40.54	4707.6	1.4	22.4	0.2	0.05	99.4
26	KC	2617.5	13.86	31.32	5305.3	2.0	3.4	0.2	0.07	206.5
27		2918.6	15.45	34.92	5009.8	1.7	3.6	0.2	0.07	215.6
28		3274.9	17.34	39.18	4659.9	1.4	3.8	0.2	0.08	224.0
29		3739.2	19.80	44.74	4204.1	1.1	4.0	0.2	0.09	232.1
30	RR-ORC	5725.0	17.35	44.92	6558.3	1.1	12.1	0.3	0.03	83.4
31		6240.4	18.92	48.97	6051.7	1.0	11.6	0.3	0.03	92.7

**Table 9**  
Pressure and temperature conditions of each stream for the best cycles in terms of NPV.

4	ORC+Dryer	Stream	1	2	3	4	-	-	-	-	-	-	-
	Cyclopentane	T (°C)	60.0	60.5	140.0	93.0	-	-	-	-	-	-	-
	@150°C	P(bar)	1.4	8.0	8.0	1.4	-	-	-	-	-	-	-
10	ORC	Stream	1	2	3	4	-	-	-	-	-	-	-
	Cyclopentane	T (°C)	60.0	61.0	170.0	99.8	-	-	-	-	-	-	-
	@180°C	P(bar)	1.4	16.0	16.0	1.4	-	-	-	-	-	-	-
12	RORC	Stream	1	2-1	2-2	3	4-1	4-2	-	-	-	-	-
	Cyclopentane	T (°C)	60.0	61.0	82.2	170.0	99.8	72.0	-	-	-	-	-
	@180°C	P(bar)	1.4	16.0	16.0	16.0	1.4	1.4	-	-	-	-	-
17	KC AW-90%	Stream	1	2-1	2-2	3-1	3-2	3-3	3-4	4-1	4-2	4-3	4-4
	@180°C	T (°C)	60.0	63.9	147.4	188.1	188.1	317.1	188.1	167.7	116.0	157.5	86.5
		P(bar)	23.2	119.0	119.0	119.0	119.0	119.0	119.0	23.2	23.2	23.2	23.2
21	TLC - 245ca	Stream	1	2	3	4	-	-	-	-	-	-	-
	@180°C	T (°C)	60.0	62.3	170.0	60.0	-	-	-	-	-	-	-
		P(bar)	3.3	37.0	37.0	3.3	-	-	-	-	-	-	-
30	RR-ORC	Stream	1	2-1	2-2	2-3	3	4-1	4-2	-	-	-	-
	Cyclopentane	T (°C)	60.0	61.0	107.8	167.9	200.0	132.9	72.0	-	-	-	-
	@180°C	P(bar)	1.4	16.0	16.0	16.0	16.0	1.4	1.4	-	-	-	-

**Table 10**  
Economics and emission indicators for positive NPV WHR alternatives.

	WHR Alternative	Economics				Emissions	
		TCC [MUSD]	i% (return)	PB [y]	NPV [MUSD]	SIC [\$/W]	Em SIN [tonnes CO2/y]
0	ORC	7.42	11.5	7.4	27.9	3484.4	3917.8
1		7.67	13.1	6.6	34.7	2959.6	4765.7
2		10.65	8.9	9.0	27.1	3230.2	6066.0
3		8.23	12.8	6.8	36.2	2365.0	6404.2
4	ORC+Dryer	9.76	9.5	8.6	27.6	2804.8	6818.1
5	KC	13.05	2.7	15.2	4.3	5742.7	4179.2
6		15.59	3.0	14.7	6.2	6002.1	4779.7
7		16.60	3.9	13.6	10.4	5651.3	5402.8
8		16.98	5.0	12.4	16.4	5140.1	6075.6
9	ORC	9.12	10.2	8.1	28.7	2725.8	6157.4
10		11.46	10.3	8.0	36.8	3039.6	6936.4
11	ORC+Dryer	13.05	7.9	9.7	27.5	3460.0	7540.9
12	R-ORC	8.14	15.6	6.1	42.4	1985.7	7543.2
13	KC	18.22	2.9	14.9	6.8	6261.6	5353.9
14		15.80	5.5	11.8	18.2	4835.1	6012.7
15		17.03	6.1	11.3	23.1	4664.4	6717.4
16		17.54	7.1	10.3	31.2	4282.4	7532.6
17		19.74	7.5	10.0	38.5	4217.3	8609.7
18	TLC	9.83	3.7	13.9	5.5	4633.0	3902.8
19		9.14	4.5	12.9	7.3	4128.0	4074.0
20		9.71	4.1	13.4	6.7	4381.9	4076.9
21		10.42	4.3	13.1	7.8	4572.0	4193.1
22	ORC	9.26	0.5	19.1	0.1	8579.1	1984.7
23		9.94	2.2	16.0	2.2	7218.1	2534.6
24		10.53	9.4	8.6	29.1	3651.1	5303.6
25		10.33	11.5	7.4	38.8	3049.4	6233.8
26	KC	7.59	10.2	8.1	23.8	2901.4	4815.2
27		11.31	7.1	10.3	20.0	3874.0	5369.0
28		11.98	8.0	9.6	25.7	3657.4	6024.5
29		15.05	7.5	10.0	29.4	4024.0	6878.7
30	RR-ORC	8.69	17.3	5.1	56.5	1518.3	10531.7
31		10.72	18.3	4.9	74.7	1718.1	11479.9

the inlet and outlet of the expander, VFR, and the net work delivered by the cycle,  $\dot{W}_{net}$ , against  $\Delta T$  which is the temperature difference between the working fluid critical temperature and its temperature before entering the expander. The horizontal dotted line represents (VFR = 50), which is the maximum VFR that a single-stage expander could properly handle, according to [50]. When the outlet temperature of the heat source gases is held at 120 °C in the evaporator, all working fluids comply with VFR values under such a limit; however,  $\dot{W}_{net}$  is lowest when compared to higher temperatures. The crossover of VFR values with the dotted line starts when the temperature is raised to 150 °C; here, the R365mfc is discarded. At 180 °C, the best  $\dot{W}_{net}$  values are obtained. However, three working fluids are discarded due to the same criterion, R365mfc, pentane, R141b, all exhibit a VFR > 50.

From the point of view of the delivered  $\dot{W}_{net}$ , the best performance, 2279.3 kW, is obtained using R245ca. But with a VFR = 41.9, that makes the R21 stand out, with  $\dot{W}_{net}$  = 2203 kW and a 39.4% lower VFR than R245ca of just 24.73. The TLC point with R21 at 180 °C looked very promising for its high  $\dot{W}_{net}$  and lowest VFR of all settings at that temperature. However, it was ruled out when analysed from an economic point of view since it had a negative NPV. This is because it is the one with the highest BWR (0.24) of all the configurations analysed, including ORC and Kalina. A high BWR means that the power consumed by the pump is relatively large relative to the work generated by the turbine, which implies a much larger pump size than in the rest of the configurations. Finally, the further the temperature of the working fluid at the inlet of the expander is from its critical temperature, the delivered

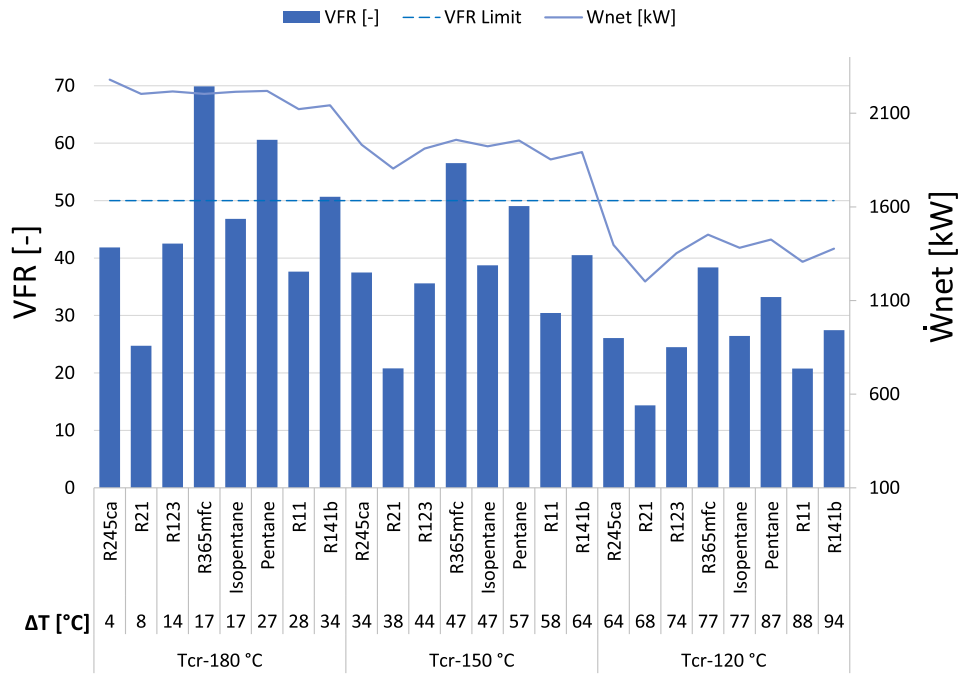


Fig. 6. VFR and  $\dot{W}_{net}$  for TLC.

$\dot{W}_{net}$  heavily decreases. Such a trend is in agreement with the results presented in [46].

Points 18–21 in Table 8 present the set-up and performance indicator of the TLCs with positive NPV. The delivered net work is very similar among such configurations varying in a small range from 2122 kW for R11 to 2279 kW for R245ca. This is attributable to the very essence of the TLC, which is the expansion from the saturated liquid into two phases. Such a constraint limits the energy input that the working fluid can handle before starting the phase change. This influences the thermal and exergy efficiency of the cycles, the latter being between 21.11% and 22.68% for the working fluids mentioned above. Then, it could be said that if there is not a very large volume change in the expander,  $VFR > 50$ , the exergy performance of the TLC is independent of the working fluid. Likewise, for those cycles where the NPV is positive, generally, when the critical temperature of the working fluid is closer to the source temperature, the economic performance will also be independent of the working fluid, and it can be limited between a SIC of 4633 \$/kW with NPV of 0.055 MUSD for R11 and a SIC of 4572 with VPN of 0.078 MUSD for R245ca. Now, between configurations, the decisive criterion will be either the VFR or the “size” of the cycle. In both cases, the less, the better. Thus, in terms of VFR, the R11 constitutes the best alternative to TLC. However, the size of a power cycle is a bit more complex to explain and can be understood in two ways, like this: (1) smaller equipment or (2) lower mass flow of working fluid. Lower SP leads to smaller expander size, lower BWR, smaller pump size. Among the cycles studied with a positive NPV, the TLC has the largest BWR, being as high as 0.21 for R11.

In Table 8, the mass flow rate of working fluid is normalised to net work and is called the Normalised net work,  $N\dot{W}_{net}$ . A higher value implies a more compact cycle [52]; thus, for the TLC, the indicator is more telling than the VFR itself, while the difference between alternatives is more pronounced. The least compact TLC operates with R11 and an  $N\dot{W}_{net}$  of 10.3, while the most compact is the one that uses Isopentane with an  $N\dot{W}_{net}$  of 31.0; this is approximately three times the variation in size against a mere 2.8% in the delivered net work. The incidence of the  $N\dot{W}_{net}$  will be explored in Section 3.4.

#### Kalina cycle

Among all the cycles, it is striking that the KC is the one with the highest  $N\dot{W}_{net}$  according to [52]. A higher value implies a more compact cycle since this indicator is related to the working fluid’s mass flow, which, in turn, is directly related to the size of the working fluid storage tank. In this work, the best performing KC has a  $N\dot{W}_{net}$  value of 232, which is much higher than any of the other technologies evaluated Table 8, which shows a smaller space occupied by the storage tank. Regarding the expander size parameter SP, in the KC, it remains in the range of 0.2–0.3 m, the same interval as the other cycles evaluated. Therefore, the size of the expanders for all cycles is relatively similar.

When analysing the BWR, smaller values indicate a smaller pump size. The best KC in terms of thermodynamic performance (point 17) had a BWR of 0.09, compared with the BWR of the best ORC, R-ORC, and RR-ORC (points 10, 12, 31 respectively), which for all cases was 0.03. The KC was three times higher, implying a much larger pump in this cycle than for all the ORC variants. However, it remains smaller than the pump size of the best TLC (point 21), which displays a BWR of 0.18. Thus, although the KC has a more significant mass flow than the ORC, the high pressure that this cycle demands requires a much higher pump capacity.

Regarding costs Fig. 8, point 17 shows the best NPV among KCs, 0.385 MUSD with a SIC of 4217.3\$/kW. However, this point has the highest total capital cost (TCC) of all alternatives, 0.1974 MUSD. This high cost of capital could pose an obstacle if this technology is to be implemented due to budget constraints. Moreover, when compared to point 28 (TCC = 0.257 MUSD, SIC = 3657.4 \$/kW and TCC = 0.1198 MUSD), the NPV gain of choosing point 17, roughly 33%, is overshadowed by the 65% increase.

#### Exergy destroyed by component

Fig. 7 shows the exergy destroyed by the components of the power cycles evaluated in this work, RR-ORC, TLC, KC, and the WHR alternatives from [35], ORC, ORC+Dryer, R-ORC, with positive NPV. Points in Fig. 7 hold the same notation as Tables 7 and 8, depicting the WHR

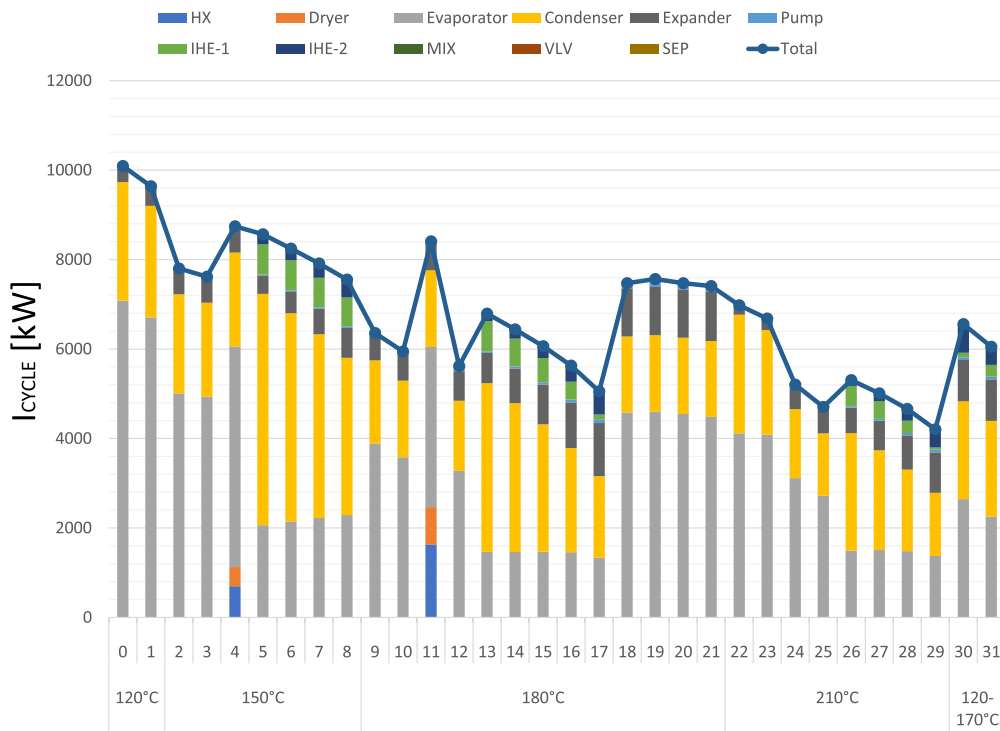


Fig. 7. Exergy destroyed by component of the cycle.

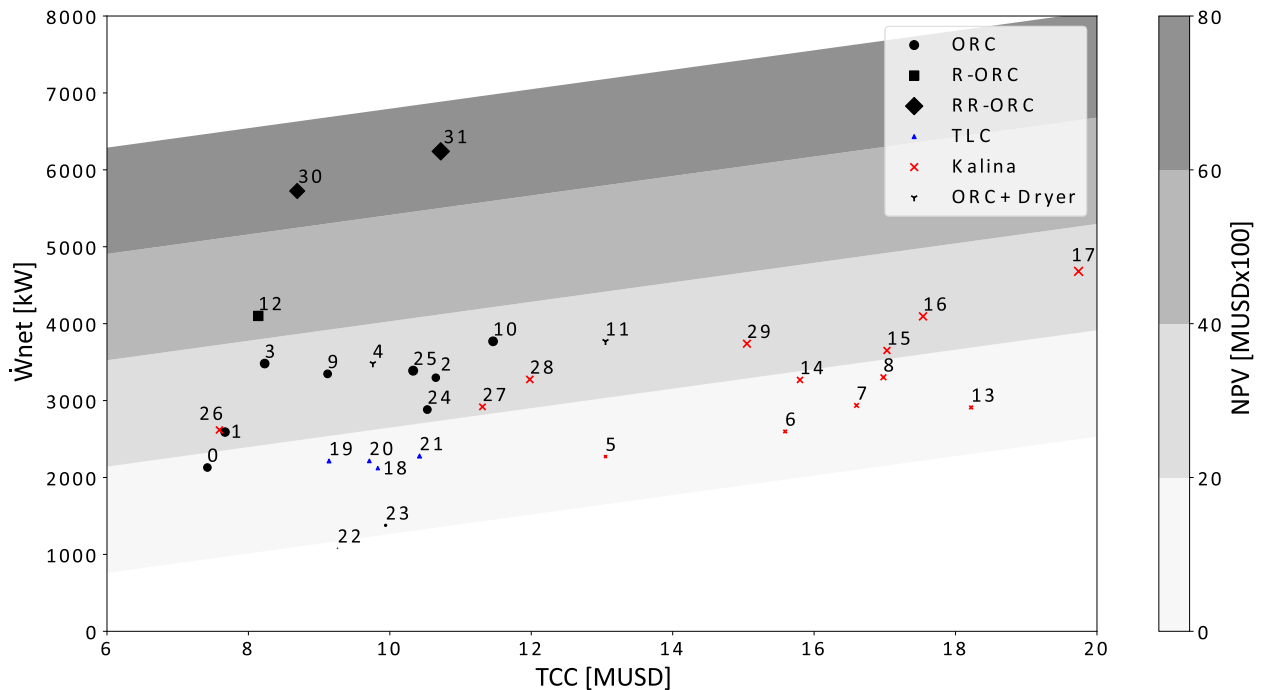


Fig. 8. NPV as a function of TCC and  $\dot{W}_{net}$ . Marker size increases with NPV.

set-ups by power cycle family and the temperature of the heat source after passing through it. A trend is observed that higher temperatures imply higher thermal and exergy efficiency of the cycles and lesser total exergy destruction. Most of the exergy is destroyed in the evaporator, followed by the condenser, since these components exhibit higher irreversibilities due to the heat transfer nature. In the basic ORC and TLC, the evaporator accounts for >50% of all destroyed exergy, and the condenser for >20%.

For the expander, higher temperatures come with higher destroyed

exergy. In ORCs and TLC, the expander represents between 3–15% of the total exergy destroyed, increasing according to temperature. In the Kalina cycle, the exergy destroyed in this component is much higher, 5–23%. It also depends on the composition of the ammonia-water mixture. The greater the concentration of ammonia, the greater the exergy destroyed by the expander due to the larger flow rate. In all cycles, the exergy destruction attributable to the pump is very low, around just 1% of the total. Exergy destroyed by separators, mixers, and valves is negligible.

The presence of an IHE decimates the amount of total destroyed exergy by the power cycle and the destroyed exergy in the evaporator. Kalina cycles are the most efficient regarding this parameter because of the better correspondence between the working fluid evaporation temperature and the heat source. The higher the ammonia content, the lower the destroyed exergy. Point (29), which operates at 90% AW at 210 °C outlet temperature, has the lowest destroyed exergy of 4.22 MW, corresponding to an EDF = 1.1; the lower the EDF, the better. In this sense, the Kalina cycle presents the best performance for the analysed temperatures, being surpassed by the RR-ORC despite destroying higher total exergy, 6 MW, at point 31. It also delivers more power, getting an EDF = 1.0. This parameter is a higher decision criterion than the exergy destroyed by the cycle as it allows it to be individualised according to the useful exergy stream, the net work. In the TLC, points 18–21, it can be seen that if the working fluid is varied, the exergy destroyed per component remains almost unchanged. This also applies to TLC set-ups that had negative NPV. But total destroyed exergy is around 20% higher than for ORCs and Kalina at the same temperature.

Carbon dioxide emissions assessment

There are three primary sources of CO<sub>2</sub> emissions in the cement manufacturing process. The first one is the decarbonisation reaction of calcium carbonate CaCO<sub>3</sub> in the calcination stage during clinker production [67]. The second source of emissions is due to the combustion of fuels that provides thermal energy for clinkerisation. Finally, the third source is linked to the consumption of electricity within the plant for processes like crushing, grinding, homogenisation, among others [68]. In this work, the waste heat recovered from the kiln effluent gases is intended to generate electricity through a power cycle. Therefore, the CO<sub>2</sub> source that would be affected is related to electricity savings due to the implementation of a power cycle and drying in the case of the ORC+dryer.

Emission savings due to electricity generation are calculated as shown in Eq. (26), where the useful exergy ( $\dot{X}_{useful}$ ), which is equivalent to the net work ( $\dot{W}_{net}$ ), is multiplied to an emissions factor (EF). The latter is for the Colombian National Interconnected System (SIN) [69] and accounts for the emissions of the country grid, involving several energy sources like hydro, coal, gas, oil, etc. Emission savings due to the

dryer are calculated as,

$$Em = \dot{X}_{useful} * EF \tag{26}$$

where the useful exergy in the dryer, ( $\dot{X}_{useful}$ ), is multiplied by an emissions factor (EF), which is the emission factor for an average coal-fired boiler [70].

Implementing one of these power cycles does not affect the amount of clinker produced; thus, the emissions produced by the burning of fuels in the kiln and the decarbonisation reaction of the CaCO<sub>3</sub> are contained within the raw material used in the clinkerisation process and remain unaffected. Consequently, only the emissions saved due to electricity consumption were considered. Then, the cycles that save the most emissions coincide with those that deliver the most net work. Moreover, the increase in fan power consumption because of the additional pressure decrease caused by a capturing heat exchanger in the hot gasses stream is not considered.

Fig. 9 shows the CO<sub>2</sub> emissions saved for the evaluated cycles. Among the RR-ORC configurations, the one that saves the most emissions of CO<sub>2</sub> emissions is the RR-ORC@170 °C (31). It would prevent 11479 tonnes of CO<sub>2</sub> per year from being released to the environment. On the other hand, the Kalina cycle that saved the most CO<sub>2</sub> emissions is the KC-90%@180 °C (17), with a total of emissions saved of 8609 tonnesCO<sub>2</sub>/y. Among the variants of the R-ORC cycles, the best configuration was the R-ORCCyclo-Pentane @180°C (12) with a total emission saved of 7543 tonnesCO<sub>2</sub>/y. The best among the ORC+Dryer was the ORC+Dryer-Cyclo-Pentane@180 °C (11) configuration, with a total emission saved of 7540.94 tonnesCO<sub>2</sub>/y, of which 8% corresponds to the emissions saved due to the dryer. Among the simple ORCs, the one that saves the most emissions was the ORC-Cyclo-Pentane@180 °C (10) with 6936 tonnesCO<sub>2</sub>/y, and finally, the one that saves the most emissions among the TLC variants was the TLC-R245ca@180 °C (21) with 4193 tonnesCO<sub>2</sub>/y.

Decision making

In this work, the input variables for the ORC and TLC were: the evaporation temperature and the working fluid. For KC, it was the evaporation temperature and the ammonia-water composition. Multiple linear regression was carried out to verify if it is possible to find a model

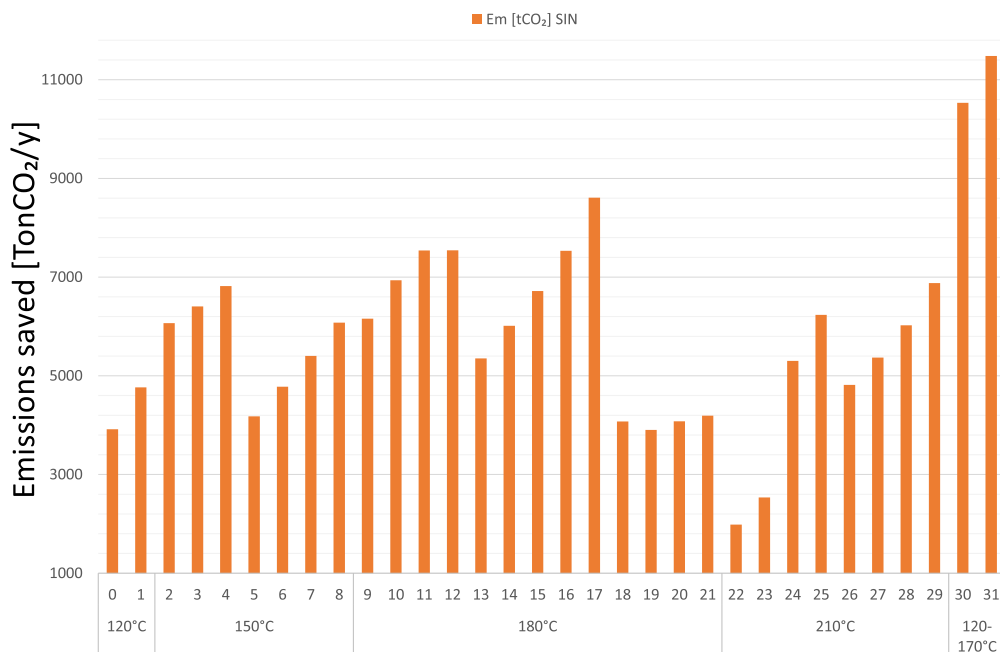


Fig. 9. Saved emissions.

that can predict the behaviour of the SIC in the face of variations in these parameters with a certain level of confidence. The working fluid in the ORC and TLC is a qualitative variable. Therefore, to make it a purely quantitative model, the fluid was replaced by its respective critical temperature and pressure ( $T_{cr}$  and  $P_{cr}$ ) of each fluid as independent variables together with the evaporation temperature. In the case of KC, the regression took the ammonia-water composition and the evaporation temperature as independent variables.

Table 11 shows the adjusted  $R^2$ , the P-value and the regression coefficients for each of the cycles. It is observed that the adjusted  $R^2$  for ORC, TLC and KC were 0.78, 0.80 and 0.76, respectively, indicating that the models adjusted for ORC and TLC can predict between 78 and 80% of the time the variability observed in the dependent variable (SIC). Regarding the P-value, for all cycles, it was  $<0.05$ ; there is a statistically significant relationship between the variables with a confidence level of 95%. In other words, the ORC and TLC parameters such as  $T_{cr}$ ,  $P_{cr}$  and  $T_{evap}$  are sufficient to predict the behaviour of the SIC between 78 and 80% of the time. In the case of the KC, Ammonia – water concentration (AW) and  $T_{evap}$  are sufficient to predict the SIC 76% of the time with a confidence level of 95%.

It should be clarified that the SIC will not be used as a decision criterion because although there is a relation between high net power production ( $\dot{W}_{net}$ ) and low specific investment cost, low SIC values and high  $\dot{W}_{net}$  are not directly equivalent objectives and therefore do not lead to the same results. Simply high values of  $\dot{W}_{net}$  and low total capital cost (TIC) can result in expensive or underperforming systems. Therefore, the primary decision criterion for this work was the NPV.

The Kalina cycle clearly shows that the SIC alone cannot be relied upon as the sole selection criterion. The lowest SIC (2901.3 \$/kW) belongs to the KC of point 26. However, this only generates a net work of 2617.52 kW and has an NPV of 0.23MUSD. On the other hand, there is point 17 that has a higher SIC (4217.29 \$/kW), but at the same time a net work of 4680 kW which is the highest of all the KC configurations and has an NPV of 0.38 which is the highest of all KC configurations. In this case, according to the SIC, the best alternative would be that of point 26. However, if what matters is to have a high output power and is analyzed from the point of view of the net present value, point 17 is the most profitable. The authors [53] confirm that using this indicator as a final decisive criterion is not advisable.

Fig. 8 corresponds to the contour plot obtained when performing the multi-linear regression of the points with positive NPV recorded in the Table 10. The equation used to plot the contours in Fig. 8 is,

$$NPV[\text{MUSD} \times 100] = -1.832 * (\text{TCC}[\text{MUSD}]) + 0.014 * (\dot{W}_{net}[\text{kW}]) \quad (27)$$

It has a multi-linear correlation coefficient of  $R^2 > 0.9$  and a  $p$ -value  $\ll 5\%$ , which implies that the hypothesis of dependence between such variables cannot be rejected and that the dependence between them is linear. This way of representing the information allows a very quickly spotting of which would be the best solution to take advantage of a waste heat source. In this work, the source of residual heat is the exhaust gases from the rotary kiln of a cement factory. However, the heat source conditions, in temperature, 327 °C, and high mass flows, 132.4 kg/s, are transferable to other energy-intensive industries. Therefore, the analysis

**Table 11**  
Parameters and coefficients of multiple linear regression.

	ORC	TLC	KC
Adjusted $R^2$	0.78	0.80	0.76
P value	8.E–05	8.E–08	2.E–06
Intercept	5056.64	11401.55	40316.12
$T_{cr}$ [°C]	–24.75	–32.51	–
$P_{cr}$ [Bar]	116.24	1138.15	–
$T_{evap}$ [°C]	19.12	–31.32	–76.54
AW[%]	–	–	–246.57

developed in this section complements the traditional approach of infinite capital, which only considers the NPV, to more realistic scenarios and is perfectly repeatable for waste heat sources with other characteristics or restrictions, as long as the results are updated.

Three criteria are preponderant when deciding to commit more resources in the investigation or implementation of a waste heat recovery strategy. These are: the net present value, NPV, as a measure of the economic performance of a potential investment; the total cost of capital, TCC, as a budget constraint; and, the delivered net work by each alternative,  $\dot{W}_{net}$ , which is the main thermodynamic performance criterion since the total destroyed exergy is already included within the calculation of the NPV. Maintaining the assumption of using the same heat source as before, the following are potential scenarios where the best waste heat recovery strategy is readily pointed out.

- There is a specific energy requirement: either due to efficiency or improvement policies in the plant or an increase in production that compromises or takes the installed capacity to the limit in electrical energy, and a certain amount of power must be met. By way of illustration, the following aspects were considered. First, an additional  $>3000$  kW is required. The company in question can draw a horizontal line at this value and focus on those points that deliver the most power. In this case, the net work is used as the discard criterion and removes the TLC from the plausible alternatives. The second criterion to consider will be the total cost of capital: how much money does the company have available for this investment? If your budget constraint is at 10 MUSD, it will discard almost all Kalina cycles, which have higher capital costs due to added complexity, corrosion issues, and higher pressures. But several ORC configurations and even an ORC with a drying unit are still within this range. Finally, the company must decide if economic performance is the decisive criterion; point 30, an ORC with two IHEs, is the most straightforward option. If some other difficult-to-quantify variable is essential, i.e., alleviate the mill load of raw material by introducing less moisture using a dryer, the selection could be point 4.
- There is a strict limitation on costs: an efficiency improvement must be introduced in the process, but the available budget is tight. Only 8 MUSD are available for investment. Therefore, most alternatives should be ruled out and remain in the hands of those that are less complex or offset capital costs efficiently. Here, points 0, 1, and 26 enter the discussion, with a very similar delivered power, between 2000–2500 kW. The simplest solution must be chosen: the ORC that delivers the highest power–point 1, which works with Cyclopentane.

If two very similar alternatives are considered, other indicators must be acknowledged; for example, the compactness of the WHR solution, the type of expander, the operating pressures, the saved emissions (as shown in Section 3.3, etc. However, those performance criteria are consigned in the table and are a sound basis for making the selection. Space is often a limitation when trying to implement a waste heat recovery system, and rarely is it considered. In plants with limited space available or if it is necessary to implement a waste heat recovery cycle onboard ships [52], having cycle size indicators becomes very important. For this reason, it is necessary to consider space as a decision variable for the implementation of one of these power cycles.

In this work, three main element size factors were considered. The VFR, which is related to the nature of the working fluid and generally favours refrigerants over alkanes; as a lower VFR implies a smaller expander. The turbine size parameter, SP, offers a first approximation to the actual size of the expander [51], where larger SP values indicate higher costs. Finally, the  $N\dot{W}_{net}$  parameter is related to the size of the working fluid storage tank; a high  $N\dot{W}_{net}$  means a small storage tank. In general terms, it is found that for a waste heat source such as the one analysed in this work, the ORC configurations with IHEs, present a

better performance than the TLC and Kalina, both in energy and exergy, as well as in costs. This is added to less complexity in operation and the utilisation of traditional, single-phase expanders.

## Conclusions

As mentioned earlier, this work was developed within a university-industry agreement framework to evaluate technical elements of WHR systems in addition to environmental considerations and economic aspects, focused on the cement industry. In general, for all the cases analysed, it can be concluded that decision-making is a complex process where many variables must be taken into account; in Fig. 8 variables are portrayed as those which are relevant for a company that desires to implement a WHR alternative. TCC and  $\dot{W}_{net}$  could be alternatively a fixed requirement, and NPV remains as the decision criterion. The presented analysis is perfectly repeatable for waste heat sources with other characteristics or restrictions, as long as the results are updated. Additionally, regarding environmental considerations, the higher the valuable exergy recovered by a WHR alternative, the higher the saved emissions.

As observed, ORCs present a better exergo-economics performance with higher released power and lower TCC. Furthermore, including IHEs improves the overall performance by pushing the expansion temperature up while allowing higher heat input to the cycle. Meanwhile, TLCs could be said that as long as there is not a very large volume change in the expander,  $VFR > 50$ , the exergy performance will be independent of the working fluid. Therefore, the delivered net-work is similar among such configurations varying in a small range. Likewise, for those cycles where the NPV is positive, generally, when the critical temperature of the working fluid is closer to the source temperature, the economic performance will also be independent of the working fluid.

Finally, the Kalina cycles exhibit the lowest total exergy destroyed among all cycles. The higher the ammonia concentration, the lower the total destroyed exergy; however, when focusing on components, the composition is linked to the exergy destroyed in the expander since there is a higher mass flow passing through it. The delivered net power falls short of compensating for the higher capital costs due to elevated operating pressures and extra complexity of the cycle, somehow making this system less attractive for WHR. Despite this, the cycle stands out for its compactness, allowing deliberation about its use in applications where space is decisive, as could be the case of existing and operating cement plants.

## CRedit authorship contribution statement

**José J. Fierro:** Validation, Investigation, Software, Investigation, Writing - original draft. **Cristian Hernández-Gómez:** Validation, Investigation, Software, Investigation, Writing - original draft. **Carlos A. Marengo-Porto:** Validation, Investigation, Software, Investigation, Writing - original draft. **César Nieto-Londoño:** Conceptualization, Methodology, Supervision, Project administration, Funding acquisition, Writing - review & editing. **Ana Escudero-Atehortua:** Conceptualization, Methodology, Writing - review & editing. **Mauricio Giraldo:** Conceptualization, Methodology, Supervision, Writing - review & editing. **Hussam Jouhara:** Conceptualization, Methodology, Supervision, Project administration, Funding acquisition, Writing - review & editing. **Luiz C. Wrobel:** Conceptualization, Methodology, Supervision, Writing - review & editing.

## Declaration of Competing Interest

The authors declare that they have no known competing financial interests or personal relationships that could have appeared to influence the work reported in this paper.

## Acknowledgements

This research is funded by the The Royal Academy of Engineering through the Newton-Caldas Fund IAPP18-19\218 project that provides a framework where industry and academic institutions from Colombia and the UK collaborate in the heat recovery in large industrial systems.

## References

- [1] Balsara S, Jain PK, Ramesh A. An integrated approach using AHP and DEMATEL for evaluating climate change mitigation strategies of the Indian cement manufacturing industry. *Environ Pollut* 2019;252:863–78.
- [2] Madlool NA, Saidur R, Rahim NA, Islam MR, Hossain MS. An exergy analysis for cement industries: An overview. *Renew Sustain Energy Rev* 2012;16:921–32.
- [3] Summerbell DL, Barlow CY, Cullen JM. Potential reduction of carbon emissions by performance improvement: A cement industry case study. *J Clean Prod* 2016;135:1327–39.
- [4] Herrera B, Amell A, Chejne F, Cacua K, Manrique R, Henao W, Vallejo G. Use of thermal energy and analysis of barriers to the implementation of thermal efficiency measures in cement production: Exploratory study in Colombia. *Energy* 2017;140 (September 2017):1047–58.
- [5] Kajaste R, Hurme M. Cement industry greenhouse gas emissions - Management options and abatement cost. *J Clean Prod* 2016;112:4041–52.
- [6] Gouardères F. Energy Policy. General Principles. tech. rep., European Parliament; 2018.
- [7] Pappatrou M, Kosmadakis G, Cipollina A, La Commare U, Micale G. Industrial waste heat: Estimation of the technically available resource in the EU per industrial sector, temperature level and country. *Appl Therm Eng* 2018;138:207–16.
- [8] Shen ZG, Tian LL, Liu X. Automotive exhaust thermoelectric generators: Current status, challenges and future prospects. *Energy Conv Manage* 2019;195(February):1138–73.
- [9] Champier D. Thermoelectric generators: A review of applications. *Energy Conv Manage* 2017;140:167–81.
- [10] Leblanc S, Yee SK, Scullin ML, Dames C, Goodson KE. Material and manufacturing cost considerations for thermoelectrics. *Renew Sustain Energy Rev* 2014;32:313–27.
- [11] Mahmoudi A, Fazli M, Morad MR. A recent review of waste heat recovery by Organic Rankine Cycle. *Appl Therm Eng* 2018.
- [12] Dolz V, Novella R, García A, Sánchez J. HD Diesel engine equipped with a bottoming Rankine cycle as a waste heat recovery system. Part 1: Study and analysis of the waste heat energy. *Appl Therm Eng* 2012;36(1):269–78.
- [13] Zhao R, Zhang H, Song S, Tian Y, Yang Y, Liu Y. Integrated simulation and control strategy of the diesel engine-organic Rankine cycle (ORC) combined system. *Energy Conv Manage* 2018;156(100):639–54.
- [14] Fierro JJ, Nieto-Londoño C, Escudero-Atehortua A, Giraldo M, Jouhara H, Wrobel LC. Techno-economic assessment of a rotary kiln shell radiation waste heat recovery system. *Therm Sci Eng Progress* 2021;23.
- [15] Laouid YAA, Kezrane C, Lasbet Y, Pesyridis A. Towards improvement of waste heat recovery systems: A multi-objective optimization of different organic Rankine cycle configurations. *Int J Thermofluids* 2021;11:100100.
- [16] Surendran A, Seshadri S. Performance investigation of two stage Organic Rankine Cycle (ORC) architectures using induction turbine layouts in dual source waste heat recovery. *Energy Conv Manage X*, 2020;6(August 2019):100029.
- [17] Yu Z, Han J, Liu H, Zhao H. Theoretical study on a novel ammonia-water cogeneration system with adjustable cooling to power ratios. *Appl Energy* 2014;122:53–61.
- [18] Ibrahim MB, Kovach RM. A kalina cycle application for power generation. *Proc ASME Turbo Expo* 1991;3.
- [19] Jonsson M, Yan J. Ammonia-water bottoming cycles: A comparison between gas engines and gas diesel engines as prime movers. *Energy* 2001;26(1):31–44.
- [20] Zhou C, Zhuang Y, Zhang L, Liu L, Du J, Shen S. A novel pinch-based method for process integration and optimization of Kalina cycle. *Energy Conv Manage* 2020;209(2):112630.
- [21] Bombarda P, Invernizzi CM, Pietra C. Heat recovery from Diesel engines: A thermodynamic comparison between Kalina and ORC cycles. *Appl Therm Eng* 2010;30:212–9.
- [22] Ambriz-Díaz VM, Rubio-Maya C, Chávez O, Ruiz-Casanova E, Pastor-Martínez E. Thermodynamic performance and economic feasibility of Kalina, Goswami and Organic Rankine Cycles coupled to a polygeneration plant using geothermal energy of low-grade temperature. *Energy Conv Manage* 2021;243(May):114362.
- [23] da Costa Horta GR, Barbosa EP, Moreira LF, Arrieta FRP, de Oliveira RN. Comparison of Kalina cycles for heat recovery application in cement industry. *Appl Therm Eng* 2021;195(January):117167.
- [24] Iglesias Garcia S, Ferreiro Garcia R, Carbia Carril J, Iglesias Garcia D. A review of thermodynamic cycles used in low temperature recovery systems over the last two years. *Renew Sustain Energy Rev* 2018;81(August 2017):760–7.
- [25] Ajimotokan HA, Sher I. Thermodynamic performance simulation and design optimisation of trilateral-cycle engines for waste heat recovery-to-power generation. *Appl Energy* 2015;154:26–34.
- [26] Iqbal MA, Rana S, Ahmadi M, Date A, Akbarzadeh A. Experimental study on the prospect of low-temperature heat to power generation using Trilateral Flash Cycle (TFC). *Appl Therm Eng* 2020;172(September). 2019, p. 115139.

- [27] Fischer J. Comparison of trilateral cycles and organic Rankine cycles. *Energy* 2011; 36(10):6208–19.
- [28] Read M, Stosic N, Smith IK. Optimization of Screw Expanders for Power Recovery From Low-Grade Heat Sources. *Energy Technol Policy* Jan 2014;1:131–42.
- [29] Bianchi G, Kennedy S, Zaher O, Tassou SA, Miller J, Jouhara H. Two-phase chamber modeling of a twin-screw expander for Trilateral Flash Cycle applications. *Energy Procedia* 2017;129:347–54.
- [30] Imran M, Usman M, Park BS, Yang Y. Comparative assessment of Organic Rankine Cycle integration for low temperature geothermal heat source applications. *Energy* May 2016;102:473–90.
- [31] Bianchi G, Marchionni M, Miller J, Tassou SA. Modelling and off-design performance optimisation of a trilateral flash cycle system using two-phase twin-screw expanders with variable built-in volume ratio. *Appl Therm Eng* 2020;179 (November). 2019, p. 115671.
- [32] Yari M, Mehr AS, Zare V, Mahmoudi SM, Rosen MA. Exergoeconomic comparison of TLC (trilateral Rankine cycle), ORC (organic Rankine cycle) and Kalina cycle using a low grade heat source. *Energy* 2015;83:712–22.
- [33] Smith IK, Stosić N, Aldis CA. Development of the trilateral flash cycle system. Part 3: The design of high-efficiency two-phase screw expanders. *Proc Inst Mech Engineers Part A J Power Energy* 1996;210(1):75–92.
- [34] Walraven D, Laenen B, D'Haeseleer W. Comparison of thermodynamic cycles for power production from low-temperature geothermal heat sources. *Energy Conv Manage* 2013;66:220–33.
- [35] Fierro JJ, Escudero-Atehortua A, Nieto-Londoño C, Giraldo M, Jouhara H, Wrobel LC. Evaluation of waste heat recovery technologies for the cement industry. *International Journal of Thermofluids* 2020;7–8:100040.
- [36] Xu J, Yu C. Critical temperature criterion for selection of working fluids for subcritical pressure Organic Rankine cycles. *Energy* 2014;74(C):719–33.
- [37] Knudsen T, Clausen LR, Haglind F, Modi A. Energy and exergy analysis of the Kalina cycle for use in concentrated solar power plants with direct steam generation. *Energy Procedia* 2014;57:361–70.
- [38] Wang Y, Tang Q, Wang M, Feng X. Thermodynamic performance comparison between ORC and Kalina cycles for multi-stream waste heat recovery. *Energy Conv Manage* 2017;143:482–92.
- [39] Júnior EPB, Arrieta MDP, Arrieta FRP, Silva CHF. Assessment of a Kalina cycle for waste heat recovery in the cement industry. *Appl Therm Eng* 2019;147:421–37.
- [40] Nag PK, Gupta AV. Exergy analysis of the kalina cycle. *Appl Therm Eng* 1998;18 (6):427–39.
- [41] Abam FI, Briggs TA, Diemuodeke OE, Ekwe EB, Ujoatuonu KN, Isaac J, Ndukwu MC. Thermodynamic and economic analysis of a Kalina system with integrated lithium-bromide-absorption cycle for power and cooling production. *Energy Rep* 2020;6:1992–2005.
- [42] Prananto LA, Zaini IN, Mahendranata BI, Juangsa FB, Aziz M, Soelaiman TAF. Use of the Kalina cycle as a bottoming cycle in a geothermal power plant: Case study of the Wayang Windu geothermal power plant. *Appl Therm Eng* 2018;132:686–96.
- [43] Wu S-Y, Zhou S-M, Xiao L, Li Y-R, Liu C, Xu J-L. Determining the optimal pinch point temperature difference of evaporator for waste heat recovery. *J Energy Inst* 2014;87(2):140–51.
- [44] Mohammadkhani F, Yari M, Ranjbar F. A zero-dimensional model for simulation of a Diesel engine and exergoeconomic analysis of waste heat recovery from its exhaust and coolant employing a high-temperature Kalina cycle. *Energy Conv Manage* Oct 2019;198:111782.
- [45] Shu G, Li X, Tian H, Liang X, Wei H, Wang X. Alkanes as working fluids for high-temperature exhaust heat recovery of diesel engine using organic Rankine cycle. *Appl Energy* 2014;119:204–17.
- [46] Chang N, Chen G. Working fluids selection from perspectives fluids selection Symposium of heat source and expander for a Trilateral cycle Assessing the feasibility of using the heat demand-outdoor Anda Song forecast Jialing for temperature function a long-term district. *Energy Procedia* 2019;158:1579–84.
- [47] Chul B, Min Y. Thermodynamic analysis of a dual loop heat recovery system with trilateral cycle applied to exhaust gases of internal combustion engine for propulsion of the 6800 TEU container ship. *Energy* 2013;58:404–16.
- [48] White MT, Read MG, Sayma AI. Using a cubic equation of state to identify optimal working fluids for an ORC operating with two-phase expansion using a twin-screw expander. In: 17th International Refrigeration and Air Conditioning Conference; 2018. p. 2172.
- [49] Angelino G, Invernizzi C, Macchi E. Organic Working Fluid Optimization for Space Power Cycles. *Mod Res Top Aerosp Propuls* 1991;297–326.
- [50] Invernizzi C, Iora P, Silva P. Bottoming micro-Rankine cycles for micro-gas turbines. *Appl Therm Eng* 2007;27:100–10.
- [51] Macchi E, Perdichizzi A. Efficiency Prediction for Axial-Flow Turbines Operating With Nonconventional Fluids. *American Society of Mechanical Engineers (Paper)* 1981;103(81-GT-15):5–11.
- [52] de la Fuente SS, Greig AR. Making shipping greener: Comparative study between organic fluids and water for rankine cycle waste heat recovery. *J Marine Eng Technol* 2015;14(2):70–84.
- [53] van Kleef LM, Oyewunmi OA, Markides CN. Multi-objective thermo-economic optimization of organic Rankine cycle (ORC) power systems in waste-heat recovery applications using computer-aided molecular design techniques. *Appl Energy* 2019;251(October 2018). p. 112513.
- [54] Bejan A, Tsatsaronis G, Moran M. *Thermal design and optimization*. John Wiley & Sons; 1996.
- [55] Pan M, Lu F, Zhu Y, Huang G, Yin J, Huang F, Chen G, Chen Z. Thermodynamic, exergoeconomic and multi-objective optimization analysis of new ORC and heat pump system for waste heat recovery in waste-to-energy combined heat and power plant. *Energy Conv Manage* Oct 2020;222:113200.
- [56] Feili M, Ghaebi H, Parikhani T, Rostamzadeh H. Exergoeconomic analysis and optimization of a new combined power and freshwater system driven by waste heat of a marine diesel engine. *Therm Sci Eng Progress* 2020;18.
- [57] Fiaschi D, Manfrida G, Rogai E, Talluri L. Exergoeconomic analysis and comparison between ORC and Kalina cycles to exploit low and medium-high temperature heat from two different geothermal sites. *Energy Conv Manage* Dec 2017;154:503–16.
- [58] Atmaca A, Yumrutaş R. Thermodynamic and exergoeconomic analysis of a cement plant: Part II - Application. *Energy Conv Manage* 2014;79:799–808.
- [59] Razaaly N, Persico G, Congedo PM. Uncertainty Quantification of an ORC turbine blade under a low quantile constrain. *Energy Procedia* 2017;129:1149–55.
- [60] Wilailak S, Yang JH, Heo CG, Kim KS, Bang SK, Seo IH, Zahid U, Lee CJ. Thermo-economic analysis of Phosphoric Acid Fuel-Cell (PAFC) integrated with Organic Rankine Cycle (ORC). *Energy* 2021;220:119744.
- [61] Figueira FL, Derjani-Bayeh S, Olivera-Fuentes C. Prediction of the thermodynamic properties of ammonia+water using cubic equations of state with the SOF cohesion function. *Fluid Phase Equilibria* 2011;303(1):96–102.
- [62] Rodríguez C, Palacio J, Venturini O, Lora E, Cobas V, Santos D, Dotto F, Gialluca V. Exergetic and economic comparison of ORC and Kalina cycle for low temperature enhanced geothermal system in Brazil. *Appl Therm Eng* 2013;52(1):109–19.
- [63] Ebrahimi A, Ghorbani B, Skandarzadeh F, Ziabasharhagh M. Introducing a novel liquid air cryogenic energy storage system using phase change material, solar parabolic trough collectors, and Kalina power cycle (process integration, pinch, and exergy analyses). *Energy Conv Manage* 2021;228(November). 2020, p. 113653.
- [64] Zhang X, He M, Zhang Y. A review of research on the Kalina cycle. *Renew Sustain Energy Rev* 2012;16(7):5309–18.
- [65] Enick RM, Donahey GP, Holsinger M. Modeling the high-pressure ammonia-water system with WATAM and the Peng-Robinson equation of state for kalina cycle studies. *Ind Eng Chem Res* 1998;37(5):1644–50.
- [66] Soltani M, Nabat MH, Razmi AR, Dusseault MB, Nathwani J. A comparative study between ORC and Kalina based waste heat recovery cycles applied to a green compressed air energy storage (CAES) system. *Energy Conv Manage* 2020;222 (April):113203.
- [67] Costa FN, Ribeiro DV. Reduction in CO<sub>2</sub> emissions during production of cement, with partial replacement of traditional raw materials by civil construction waste (CCW). *J Clean Prod* 2020;276:123302.
- [68] León-Velez A, Guillén-Mena V. Energía contenida y emisiones de CO<sub>2</sub> en el proceso de fabricación del cemento en Ecuador. *Ambiente Construido* 2020;20:611–25.
- [69] Madri MB, Fl HH, Gonz YP. *Inconectado Nacional Colombia-Sin. tech. rep., UPME*; 2017.
- [70] Zhang Q, Yi H, Yu Z, Gao J, Wang X, Lin H, Shen B. Energy-exergy analysis and energy efficiency improvement of coal-fired industrial boilers based on thermal test data. *Appl Therm Eng* Nov 2018;144:614–27.